

## Relaxation dynamics in plastic crystals

R. Brand, P. Lunkenheimer,<sup>a)</sup> and A. Loidl

*Experimentalphysik V, Universität Augsburg, Universitätsstrasse 2, D-86135 Augsburg, Germany*

(Received 1 October 2001; accepted 19 March 2002)

We report dielectric data on six different plastic crystalline materials, namely 1-cyanoadamantane, adamantanone, pentachloronitrobenzene, cyclo-hexanol, ethanol, and meta-carborane, covering a frequency range of up to 14 decades and up to 20 GHz. Information on phase transitions, the  $\alpha$ -relaxation, and relaxation processes beyond the  $\alpha$ -relaxation are provided. The  $\alpha$ -relaxation shows clear non-Debye behavior and varying degrees of deviation from thermally activated behavior. Our results reveal a generally rather low fragility of plastic crystals. In some of the investigated materials evidence for Johari–Goldstein type  $\beta$ -relaxations is obtained. In addition, the question of the so-called excess wing of the  $\alpha$ -relaxation peak is addressed in detail. In all cases, it is either absent or can be ascribed to a  $\beta$ -relaxation submerged under the  $\alpha$ -peak. Overall, the present work provides a broad database on the dielectric behavior of plastic crystals, and may be taken as a review of the dynamic phenomena occurring in these materials, many of them being observed also in structural glass formers. © 2002 American Institute of Physics.  
[DOI: 10.1063/1.1477186]

### I. INTRODUCTION

The physics of disordered materials is a lively subfield of condensed matter physics. An especially challenging problem is the understanding of the glass transition with its tremendous, but continuous slow down of molecular dynamics when approaching the glass state.<sup>1,2</sup> Consequently many experimental investigations have focused on the investigation of the relaxation dynamics of glass-forming liquids and considerable experimental advances have allowed to investigate their very rich dynamic behavior in great detail.<sup>2,3</sup> Aside of the canonical glasses, during recent years the so-called plastic crystals have attracted considerable interest.<sup>4–11</sup> In plastic crystals the centers of mass of the molecules form a regular crystalline lattice but the molecules are dynamically disordered with respect to their orientational degrees of freedom (Fig. 1). Such a behavior was first proposed in 1924 for hydrogenchloride.<sup>12</sup> Most plastic crystals are formed by molecules of more or less globular shape, providing little steric hindrance for reorientational processes. This often causes a high plasticity, a property that led to the term “plastic crystal,” first introduced by Timmermans<sup>13</sup> many decades ago. Due to their translational symmetry, plastic crystals are much simpler to treat in theoretical and simulation approaches of the glass transition and therefore these materials are often considered as model systems for structural glass formers. Indeed the orientational relaxation dynamics of plastic crystals in many respects resembles the relaxation dynamics of conventional glass formers.<sup>14–16</sup> Especially, in many cases by sufficiently fast cooling, the high-temperature dynamically disordered state can be supercooled, thus avoiding complete orientational ordering often occurring at low temperatures. For low temperatures, below an “orientational glass temperature”  $T_g^o$ , finally a “glass-like” orientationally

disordered state (sometimes called “glassy crystal”<sup>17</sup>) that is static on all practical time scales is reached (Fig. 1). Concomitantly the dynamics shows the continuous slowing down over many orders of magnitude that is typical also for glass-forming liquids. Consequently it seems reasonable to use the term “orientational glass” for the supercooled plastic crystalline state below  $T_g^o$ . However, it should be mentioned that in literature this term sometimes is used to exclusively denote the orientationally disordered state of mixed crystals, which is believed to be caused by frustrated interactions due to substitutional disorder.<sup>11,18</sup> In contrast to these materials, the orientational-glass state in plastic crystals is nonergodic, i.e., after sufficiently (often inaccessibly) long aging times the material is expected to arrive at a completely (positionally and orientationally) ordered state. In this respect the orientationally disordered state of plastic crystals represents the true analog of the supercooled liquid and glassy state of conventional glass formers, quite in contrast to the “orientational glass” state of mixed crystals.

Due to the extremely broad dynamic range accessible (more than 19 decades<sup>3</sup>), dielectric spectroscopy has proven to be an important tool for the investigation of the relaxational response as well as in structural glass formers as in plastic crystals. Especially for the latter it is ideally suited, as the electric field directly couples to the orientational degrees of freedom. Prerequisite, of course, is the presence of a dipolar moment. Recent experimental work on ethanol, which can be prepared in both a plastic crystalline and a supercooled liquid state, revealed the importance of orientational processes also in conventional glass formers.<sup>19</sup> However, translational dynamics, which is only indirectly probed by dielectric spectroscopy, certainly also plays an important role in these materials. As in conventional glass formers, dielectric spectra of plastic crystals are dominated by the  $\alpha$ -relaxation process, showing up as a peak in the frequency-

<sup>a)</sup>Electronic mail: peter.lunkenheimer@physik.uni-augsburg.de

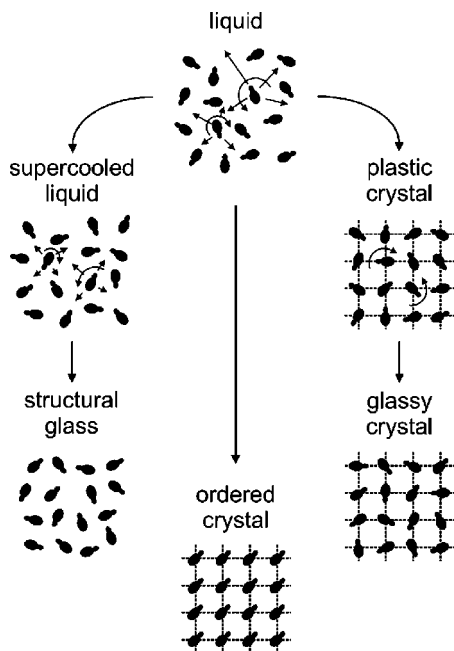


FIG. 1. Schematic representation of the possible transitions of a liquid of dipolar molecules (represented by asymmetric dumbbells) into a structural glass, an ordered crystal, or a glassy crystal.

dependent dielectric loss,  $\epsilon''$ . Its tremendous shift towards low frequencies with decreasing temperature directly mirrors the continuous slowing down of the reorientational motions of the molecules when approaching the glass temperature. Aside of the  $\alpha$ -process a variety of faster dynamic processes are known in conventional glass formers, all detectable by dielectric spectroscopy.<sup>3</sup> Among them are secondary or  $\beta$ -relaxations, the excess (or high-frequency) wing, the fast  $\beta$ -process, and the boson peak, all being not well understood until now and controversially discussed. It is commonly felt that understanding the microscopic origins of these processes is prerequisite to understanding the glass transition and glass state in general. Unfortunately these processes have only rarely been investigated in plastic crystals until now and it can be hoped that from the investigation of their presence and properties in this class of materials valuable information on their microscopic origin also in structural glass formers can be gained. But also information of the  $\alpha$ -relaxation in plastic crystals often is somewhat sparse and warrants further examination.

In the present work we provide dielectric data on six different plastic crystalline materials, covering a frequency range of up to 14 decades and up to 20 GHz. The materials investigated are 1-cyanoadamantane, adamantanone, pentachloronitrobenzene, cyclo-hexanol, ethanol, and meta-carborane. Various dielectric investigations of these materials have been reported earlier, but unfortunately only in a few cases were actual spectra shown and often the measurements were performed in restricted frequency and temperature ranges only. Also in most earlier dielectric investigations of plastic crystals the results were not represented in a way that allows for the detection and analyses of processes beyond the  $\alpha$ -relaxation. We have performed measurements in an extended frequency and temperature range, with sufficient reso-

lution to allow for a representation of the loss spectra in a double-logarithmic representation.

The investigated materials show varying abilities to supercool the plastic phase and partly phase transitions are observed involving partial orientational order. In all cases, the dynamics is governed by the  $\alpha$ -relaxation, showing clear non-Debye behavior and varying degrees of deviation from thermally activated behavior. Partly, additional relaxation processes occur. The question of the so-called excess wing, corresponding to an excess contribution on the high-frequency side of the  $\alpha$  loss-peak and well established for a number of structural glass formers,<sup>3,10,20–23</sup> is addressed in detail. The results on the fast  $\beta$ -process and the boson peak will be covered in a coming publication.<sup>24</sup> Overall, the purpose of the present work is to provide a broader database on the dielectric behavior of plastic crystals than presently available, with special emphasis on processes beyond the  $\alpha$ -relaxation. We also will address the question if the relaxational dynamics of plastic crystals reveals properties that are characteristic for this group of disordered materials and therefore must be connected to the translational order, missing in the supercooled liquids.

## II. EXPERIMENTAL DETAILS

To record the real and imaginary part of the dielectric permittivity in a broad frequency range, the combination of a variety of different techniques is necessary. In general at low frequencies,  $\nu \leq 2$  GHz, the samples were prepared in parallel-plate capacitor geometry. Solid sample materials (1-cyanoadamantane, adamantanone, pentachloronitrobenzene, and meta-carborane, purchased as powder) were pressed into the form of disk-shaped platelets and covered with silver paint, forming electrodes at adjacent sides. For samples that are liquid at room temperature (cyclo-hexanol, ethanol), either disk-shaped polished stainless-steel capacitors or gold-plated glass plates were used. The plates were kept at distance with glass-fiber spacers with typical diameters of 50  $\mu\text{m}$ . Geometrical capacitances of up to 100 pF were reached.

For the lowest frequencies, down to some  $\mu\text{Hz}$ , a home-made time-domain spectrometer was used. Here the complex dielectric permittivity is calculated via a Fourier transformation of the response function.<sup>25</sup> In the region  $30 \mu\text{Hz} \leq \nu \leq 3$  MHz the so-called frequency response analysis was applied, employing a Novocontrol  $\alpha$ -analyzer or a Schlumberger SI1260 impedance analyzer in conjunction with a Chelsea dielectric interface. These measurements were supplemented at frequencies  $20 \text{ Hz} \leq \nu \leq 20$  MHz by the standard ac-bridge technique using the Hewlett-Packard LCR-meters HP4284 and HP4285. At frequencies  $1 \text{ MHz} \leq \nu \leq 1.8$  GHz the impedance analyzer HP4291 was employed using a reflectometric technique, with the sample mounted at the end of a 7 mm coaxial line.<sup>26</sup> Finally, at frequencies up to 25 GHz measurements were taken in transmission geometry: A HP8510 network analyzer measures the transmission properties of a 7 mm coaxial line, filled with the sample material. For liquid samples the ends of the line are sealed by thin Teflon disks; solid (powder) samples were filled into the line and compressed using special pressing tools.

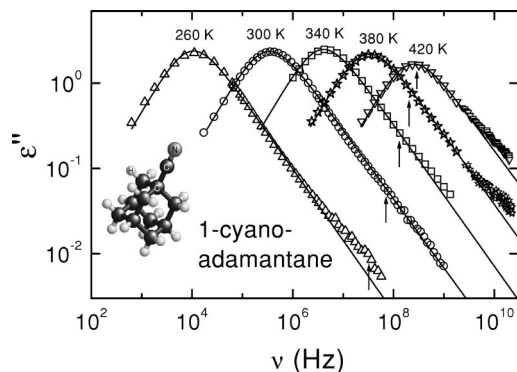


FIG. 2. Dielectric loss spectra of 1-cyanoadamantane for various temperatures. The lines are fits with the CD function, Eq. (1). The arrows indicate the  $\beta$ -peak positions calculated from an extrapolation of  $\tau_{\beta}(T)$  of Ref. 39. A schematic view of the molecular structure of 1-cyanoadamantane is shown as an inset.

For cooling and heating of the samples, a closed cycle refrigerator and a nitrogen gas-heating system were used. All materials investigated were measured as purchased without further purification. The specified purities were Adamantanone, 1-cyanoadamantane, cyclo-hexanol, and pentachloronitrobenzene:  $\geq 99\%$ ; ethanol:  $\geq 99.9\%$ ; and meta-carborane:  $\geq 98\%$ . For further experimental details the reader is referred to Refs. 27 and 28.

### III. RESULTS

In the following we will show the measured dielectric loss spectra of all materials investigated and subject them to some standard evaluation procedures. The spectra are fitted, employing commonly used empirical functions, namely the Havriliak–Negami (HN) function<sup>29</sup> and its limiting cases the Cole–Cole<sup>30</sup> (CC) and Cole–Davidson<sup>31</sup> (CD) functions. In most cases the fits were performed simultaneously for the real and imaginary part of the dielectric permittivity. The real part is not shown, as, except for the value of the limiting high-frequency dielectric constant  $\epsilon_{\infty}$  (mentioned in the text), it does not provide significant additional information. The parameters resulting from the fits are shown and the relaxation times are checked for Arrhenius or Vogel–Fulcher–Tammann (VFT) behavior.<sup>32</sup>

#### A. 1-Cyanoadamantane

The molecular structure of 1-cyanoadamantane ( $C_{10}H_{15}CN$ ) is shown in the inset of Fig. 2. The carbon atoms form a cage, the free bonds being saturated by hydrogen atoms and one cyano group. This molecule is very rigid and its only internal degree of freedom, the bending motion of the  $C-C\equiv N$  group, was shown to be much too fast to have any influence in the frequency range investigated here.<sup>33</sup> 1-cyanoadamantane is a prototypical plastic crystal and has been investigated by a variety of experimental methods,<sup>6,9,11,33–40</sup> including dielectric spectroscopy in an overall frequency range from 30 mHz to 2 GHz.<sup>9,37–40</sup> Below the melting temperature ( $T_m=458$  K) the plastic phase is formed and at  $T<280$  K orientational order occurs. The plastic-crystalline state of 1-cyanoadamantane can be super-

cooled using high cooling rates. More detailed information on phase transitions and reorientational modes in this material can be found, e.g., in Refs. 11, 35, 36, and 40. In the present investigation we focus on the plastic-crystalline phase extending the measured frequency range up to 20 GHz.

Figure 2 shows the dielectric loss spectra of 1-cyanoadamantane for various temperatures (the curves at 260 and 300 K have already been shown in Ref. 9). Well-pronounced  $\alpha$ -peaks are observed shifting towards lower frequencies with decreasing temperature. Their half-widths exceeded the value of 1.13, predicted for a monodispersive Debye relaxation process. The loss peaks exhibit an asymmetric broadening at frequencies above the peak frequency  $\nu_p$ , in agreement with the findings in Refs. 38–40. The lines in Fig. 2 are fits with the CD function,<sup>31</sup>

$$\epsilon^* = \epsilon_{\infty} + \frac{\epsilon_s - \epsilon_{\infty}}{(1 + i 2\pi\nu\tau_{CD})^{\beta_{CD}}}, \quad (1)$$

which is often employed to describe the loss peaks in structural glass formers, too. We also performed fits using the Fourier transform of the Kohlrausch–Williams–Watts (KWW) function,<sup>41</sup> however, leading to somewhat worse agreement of fit and experimental data. While for  $\nu \ll \nu_p$  the loss, calculated from Eq. (1), increases linearly, for  $\nu \gg \nu_p$  it follows a power law with an exponent equal to  $-\beta_{CD}$ . In Fig. 2, some decades above the peak frequency, the experimental data exhibit weak deviations from this power law, which were not revealed in the earlier investigations.<sup>37–40</sup> It resembles the excess wing known from structural glass formers, and will be discussed in Sec. IV B.

The temperature dependence of the  $\alpha$  relaxation time  $\tau_{\alpha}$  is shown in Fig. 3 in Arrhenius representation.<sup>42</sup> In addition to the relaxation times from the present investigation, also the results from Refs. 38–40 are included. Overall,  $\tau_{\alpha}(T)$  shows marked deviations from simple thermally activated behavior. Following the evaluation in Ref. 38, below about 250 K,  $\tau_{\alpha}(T)$  is described by the empirical VFT equation (solid line in Fig. 3):

$$\tau_{\alpha} = \tau_0 \exp\left[\frac{DT_{VF}}{T - T_{VF}}\right]. \quad (2)$$

Here  $D$  is the so-called strength parameter<sup>43</sup> and  $\tau_0$  is a prefactor, typically of the order of an inverse phonon frequency. At higher temperatures a transition to Arrhenius behavior can be observed (dashed line). However, at  $T > 400$  K,  $\tau_{\alpha}(T)$  starts to decrease steeper again. In the insets of Fig. 3 the temperature dependence of the width parameter  $\beta_{CD}$  and the relaxation strength  $\Delta\epsilon = \epsilon_s - \epsilon_{\infty}$  are shown, both being effectively constant. Also  $\epsilon_{\infty}$  is nearly constant with an average value of 2.35. The somewhat reduced  $\Delta\epsilon$  at 420 K, which corresponds to the reduced peak amplitude in Fig. 2, may be ascribed to a beginning sublimation of the sample at high temperatures.

#### B. Adamantanone

Compared to 1-cyanoadamantane, in adamantanone the cyano group is replaced by an oxygen atom (see inset of Fig.



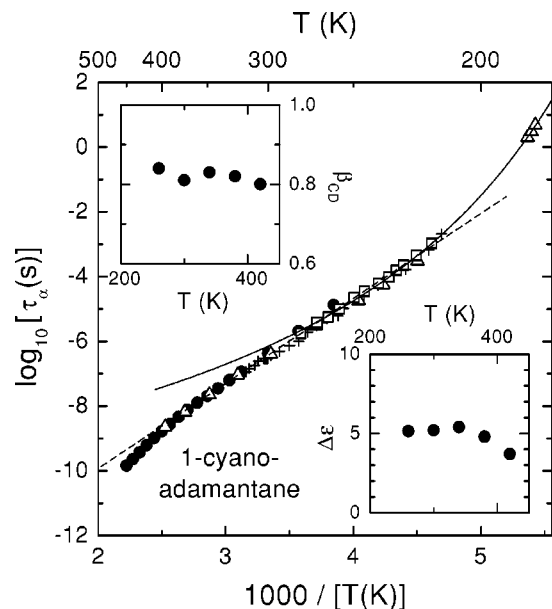


FIG. 3. Temperature dependence of the  $\alpha$ -relaxation time of 1-cyanoadamantane in Arrhenius representation [circles: present work, triangles: Amoureux *et al.* (Ref. 38), squares: Pathmanathan and Johari (Ref. 39), pluses: Tyagi and Murthy (Ref. 40)]. The solid line shows a fit with the VFT law, Eq. (2), at  $T < 250$  K; the dashed line is an Arrhenius fit at  $T > 250$  K. The insets show the power-law exponent of the high-frequency flanks of the  $\alpha$ -peaks,  $\beta_{CD}$ , and the relaxation strength  $\Delta\epsilon$  obtained from the CD fits shown in Fig. 2.

4). As the oxygen atom has a double bond to the cage, adamantanone is even more rigid than 1-cyanoadamantane. In addition, it is more close to a globular shape. As for 1-cyanoadamantane, a plastic phase (phase I) is formed below the melting point,  $T_m = 529$  K. At 178 K, adamantanone is reported to show a transition from the plastic phase into a phase, which was assumed to comprise complete orientational order (phase II).<sup>44,45</sup> The plastic phase of adamantanone has been investigated by a variety of experimental methods,<sup>44–46</sup> including dielectric spectroscopy between 5 Hz and 20 GHz.<sup>45</sup> Unfortunately, in the latter work no spectra, only the peak frequencies, were shown.

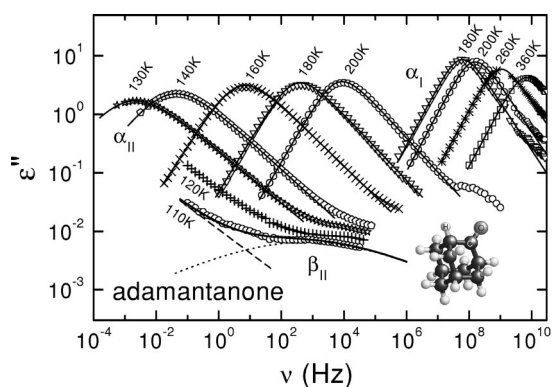


FIG. 4. Dielectric loss spectra of phase I and II of adamantanone for various temperatures. The solid lines are fits with the CD function, Eq. (1), for phase I and the HN function, Eq. (3), for phase II. The solid line through the 110 K curve is a fit with the sum of a power law (dashed line) and a CC function (dotted line). The inset shows a schematic view of the molecular structure of adamantanone.

Figure 4 shows the dielectric loss spectra in adamantanone in both phase I and II. The most intriguing result is the detection of well-pronounced loss peaks also at low temperatures, in phase II. The transition between both phases shows a considerable hysteresis and therefore, between 180 and 200 K, spectra could be collected in both phases. Obviously, the transition into phase II does not comprise complete orientational order, but presumably a partial restriction of reorientational motion, accompanied by a strong slowing down of the  $\alpha$ -relaxation. As the amplitude of the relaxation peaks is not reduced dramatically at the transition we believe that full reorientation of the molecules still is possible in phase II, but the reorientation paths are restricted, which forces the molecules to overcome higher potential barriers and results in longer relaxation times. In phase I, the spectra can be described by the CD function, Eq. (1) (solid lines in Fig. 4). Similar to the findings in 1-cyanoadamantane (Fig. 2), small deviations from CD behavior show up at the highest frequencies. Because in phase II the loss does not increase linearly at  $\nu \ll \nu_p$ , the CD function is not suited for the description of these results. Instead the HN equation can be employed:<sup>29</sup>

$$\epsilon'' = \epsilon_\infty + \frac{\epsilon_s - \epsilon_\infty}{[1 + (i\omega\tau_{HN})^{1-\alpha_{HN}}]^\beta} \quad (3)$$

For  $\nu \ll \nu_p$ , Eq. (3) leads to a power-law increase,  $\epsilon'' \sim \nu^{1-\alpha}$  and for  $\nu \gg \nu_p$ ,  $\epsilon''$  decreases with  $\epsilon'' \sim \nu^{-(1-\alpha)\beta}$ . As seen in Fig. 4, the spectra in phase I can be well described by Eq. (3). However, at high frequencies again some deviations show up. For 200 K, a shoulder is observed around  $10^8$  Hz, a similar frequency as the  $\alpha$ -relaxation peak in phase I. It can be ascribed to a partial transition of the material into phase I, which under heating starts just at 200 K. However, the deviations of fits and experimental data observed at lower temperatures cannot be explained in that way. For the lowest temperatures these deviations emerge into a shoulder, indicative of a  $\beta$ -relaxation.<sup>47</sup> Indeed, as demonstrated by the solid line through the 110 K curve, this shoulder can be fitted by a sum of a power law (for the high-frequency flank of the  $\alpha$ -peak, dashed line) and a CC function (dotted line).<sup>48</sup> For materials showing well-pronounced  $\beta$ -relaxation peaks, the latter is often found to provide a good description. It is equivalent to Eq. (3), with  $\beta_{HN} = 1$ , leading to symmetric loss peaks. While the CC function is purely phenomenological, its spectral shape is quite similar to that resulting from the assumption of a thermally activated process with a Gaussian distribution of energy barriers.<sup>49</sup>

The  $\alpha$ -relaxation times in both phases are plotted in Fig. 5 in Arrhenius representation. At the transition into phase II at about 180 K, the  $\alpha$ -relaxation slows down by more than five decades. In both phases the relaxation times follow an Arrhenius law, the parameters being noted in Table I. The parameters for phase I agree reasonably with those reported in Ref. 45. The considerably enhanced activation energy of 0.50 eV in phase II, compared to 0.15 eV in phase I, further corroborates the notion of a restriction of reorientational motion at the transition into phase II. In the upper inset of Fig. 5 the high-frequency power-law exponent of the loss peaks is shown as determined from the fits (Fig. 4). The significant

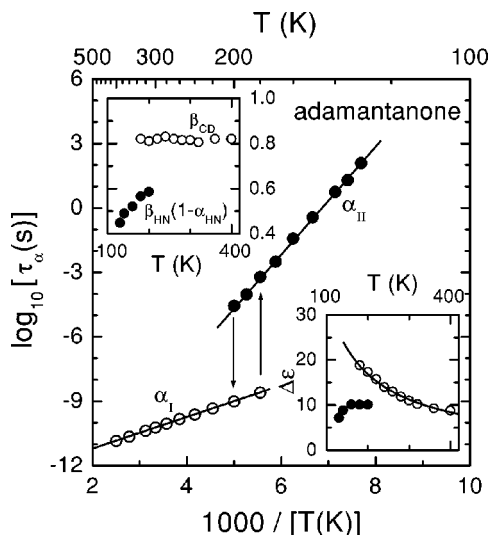


FIG. 5. Temperature dependence of the  $\alpha$ -relaxation time of adamantanone in Arrhenius representation (open circles: phase I, closed circles: phase II). The solid lines are fits with the Arrhenius law. The upper inset shows the power-law exponents of the high-frequency flanks of the  $\alpha$ -peaks as determined from the fits in Fig. 4. The lower inset shows the relaxation strength  $\Delta\epsilon$ , the line is a fit of  $\Delta\epsilon(T)$  in phase I with a Curie law.

reduction of this exponent at the transition into phase II mirrors the considerably broader loss peaks in this phase. In phase II with increasing temperature, CD behavior is approached,  $\alpha_{\text{HN}}$  decreasing from 0.37 to 0.08. As demonstrated by the line in the lower inset of Fig. 5, in phase I,  $\Delta\epsilon$  follows a Curie behavior,  $\Delta\epsilon \sim C/T$ . In Phase II,  $\Delta\epsilon$  is reduced by about a factor of 2 and constant within experimental resolution (at the lowest temperatures the error of  $\Delta\epsilon$  is large because the low-frequency wing of the  $\alpha$ -peak is only partly covered, see Fig. 4). In phase I,  $\epsilon_\infty \approx 3.75$  and in phase II,  $\epsilon_\infty \approx 3.02$ , both being approximately constant.

### C. Pentachloronitrobenzene

Many hexasubstituted benzenes show plastic phases which can be supercooled.<sup>15,16,50–52</sup> Their molecules having a

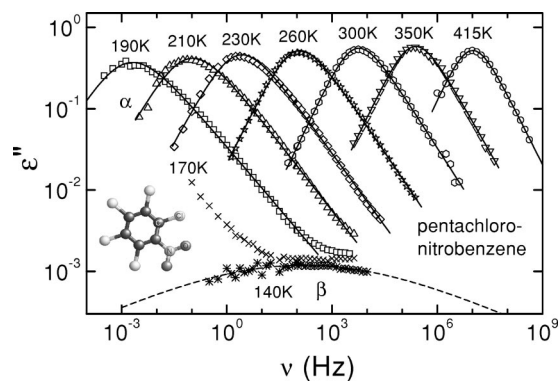


FIG. 6. Dielectric loss spectra of pentachloronitrobenzene for various temperatures. The solid lines are fits with the HN function, Eq. (3). The dashed line is a fit of the  $\beta$ -relaxation peak at 140 K with a CC function. The inset shows a schematic view of the molecular structure.

circular disk structure, the rotation is most easy about the axes perpendicular to the disk. For pentachloronitrobenzene (see inset of Fig. 6 for a sketch of the molecular structure) from dielectric investigations a plastic phase was reported above 223 K extending well up to the melting point of 415 K.<sup>50–52</sup> Those measurements covered a relatively restricted overall frequency range of 20 Hz to 1 MHz and temperatures between 175 and 430 K. They did not reveal any results on processes beyond the  $\alpha$ -relaxation.

The dielectric loss spectra of pentachloronitrobenzene are presented in Fig. 6. From 190 K well up to the melting point, the typical  $\alpha$ -peaks are observed, continuously shifting through the frequency window. The reduced peak amplitude at 415 K can be ascribed to the beginning melting process. There is no indication of full or partial orientational order attained under cooling. Especially we found no indication for the earlier-reported discontinuity in the temperature-dependent dielectric constant  $\epsilon'(T)$  (not shown) at 223 K that was interpreted assuming orientational order below this temperature.<sup>50</sup> Except for the highest temperatures, the loss exhibits a nonlinear increase at  $\nu \ll \nu_p$  and consequently the HN formula, Eq. (3), was used to fit the experimental data

TABLE I. Relaxation parameters of the plastic crystalline materials investigated in the present work. The substances are abbreviated as follows: 1-cyanoadamantane (CNA), adamantanone (AON), pentachloronitrobenzene (PCNB), cyclo-hexanol (CHEX), and meta-carborane (M-CA).  $T_{\text{VF}}=0$  denotes Arrhenius behavior.  $B$  is equal to  $DT_{\text{VF}}$  in the case of VFT behavior and  $B=E/k_B$ , with  $E$  the activation energy, in the case of Arrhenius behavior.  $T_g^o$  is the “orientational glass temperature,” determined from  $\tau(T_g^o)=100$  s.

Substance	Process	$\tau_0$ (s)	$B$ (K)	$T_{\text{VF}}$ (K)	$m$	$T_g^o$ (K)
CNA	$\alpha$ , $T < 250$ K	$2.2 \times 10^{-10}$	1416	125	24	178
	$\alpha$ , $T > 250$ K	$6.7 \times 10^{-16}$	6044	0		
	$\beta^a$	$1.5 \times 10^{-11}$	1491	0		
AON	$\alpha_I$	$2.1 \times 10^{-13}$	1696	0	15	50
	$\alpha_{II}$	$5.7 \times 10^{-18}$	5784	0	19	131
PCNB	$\alpha$	$9.9 \times 10^{-17}$	7922	0	17	191
CHEX	$\alpha$ , $T \leq 160$ K	$1.0 \times 10^{-11}$	1220	110	48	151
	$\alpha$ , $T \geq 200$ K	$1.8 \times 10^{-17}$	5677	0		
	$\gamma$	$7.5 \times 10^{-16}$	2736	0		
ethanol	$\alpha$	$1.1 \times 10^{-12}$	1189	62	38	99
	$\beta$	$2.9 \times 10^{-10}$	497	73		
M-CA	$\alpha$	$2.9 \times 10^{-19}$	6259	0	21	132

<sup>a</sup>Reference 39.

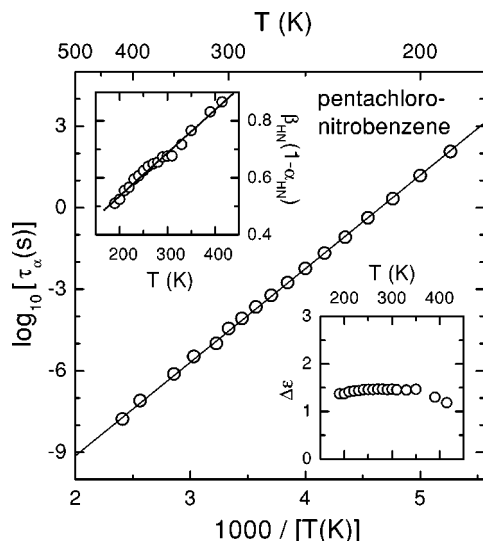


FIG. 7. Temperature dependence of the  $\alpha$ -relaxation time of pentachloronitrobenzene in Arrhenius representation. The solid line shows a fit with the Arrhenius law. The upper inset shows the power-law exponent of the high-frequency flanks of the  $\alpha$ -peaks as determined from the fits of the  $\alpha$ -peaks (Fig. 7); the line indicates linear behavior. The lower inset shows the relaxation strength  $\Delta\epsilon$ .

(solid lines in Fig. 6). At  $T \leq 230$  K, in the peak region and up to about two decades above  $\nu_p$ , the experimental curves exhibit a slightly milder curvature than the fits. It remains to be clarified if this is due to a failing of the empirical HN function or if the loss peaks may be in fact composed of two separate peaks in this region. The more pronounced deviations of experimental data and fits showing up, e.g., at about 1 kHz and 190 K can be ascribed to a weak, so-far unknown  $\beta$ -relaxation that is clearly revealed in the low-temperature result of 140 K shown in Fig. 6. For the higher temperatures this relaxation peak shifts to higher frequencies and cannot be resolved due to the relatively small losses and limited experimental resolution in this region.

As demonstrated in Fig. 7, the  $\alpha$ -relaxation time follows an Arrhenius behavior in the whole temperature region investigated. Its parameters (see Table I) are in reasonable agreement with those reported in Ref. 50. The high-frequency power-law exponent of the loss peaks shown in the upper inset of Fig. 7 increases nearly linearly with temperature. The slight anomaly near 300 K presumably is an artifact due to small matching problems between the results from frequency response analysis and reflection technique, the transition frequency being about 1 MHz. As mentioned above, the power-law exponent of the low-frequency wing of the  $\alpha$ -peak approaches unity for high temperatures,  $\alpha_{HN}$  decreasing from 0.3 to 0.05. In the lower inset of Fig. 7 the relaxation strength is shown. It is approximately constant, except for a decrease observed above 370 K, which can be ascribed to a beginning sublimation of the sample at high temperatures. Also  $\epsilon_\infty$  is nearly constant with  $\epsilon_\infty \approx 2.80$ .

#### D. Cyclo-hexanol

Already in the pioneering work by Timmermans,<sup>13</sup> cyclo-hexanol was identified as plastic crystal and it was this

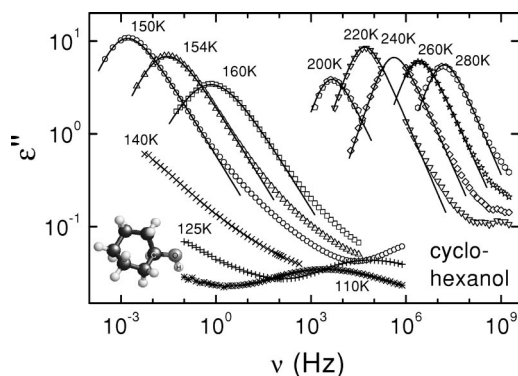


FIG. 8. Dielectric loss spectra of cyclo-hexanol for various temperatures. The lines are fits with the CD function, Eq. (1), for  $T \geq 200$  K and with the HN function, Eq. (3), for  $T \leq 160$  K. The inset shows a schematic view of the molecular structure.

material to which the term “glassy crystal” was first applied.<sup>17</sup> There is a large number of investigations of this material using different techniques,<sup>17,53–59</sup> including dielectric spectroscopy.<sup>55–59</sup> For the rather complex phase diagram of cyclo-hexanol the reader is referred, e.g., to Ref. 55. In our context it is of relevance only that below the melting point of 299 K a plastic phase is formed, which transfers below about 265 K into an orientationally ordered structure. However, the orientationally disordered state can be supercooled, leading to a glassy crystal below  $T_g^o = 149$  K. A number of relaxation processes beyond the  $\alpha$ -relaxation has been detected in this material, their origin being often ascribed to intramolecular degrees of freedom of the cyclo-hexanol molecule<sup>54–56,58</sup> (see inset of Fig. 8 for the molecular structure).

In Fig. 8 the dielectric loss spectra obtained in the present work are shown. Due to the occurrence of orientational order,  $\alpha$ -peaks are observed at  $T \leq 160$  K and  $T \geq 200$  K only. The data above 200 K were taken under cooling with a moderate rate of 0.4 K/min. At 200 K the sample starts to approach orientational order, leading to a strongly reduced peak amplitude. The data below 160 K were taken after the sample was quenched from room temperature using liquid nitrogen and subsequent heating to the desired measurement temperatures. Above 150 K, again the decreasing peak amplitude indicates a successive transition into the orientationally ordered state. For  $T > 200$  K the experimental data in the peak region can be well described by the CD function, Eq. (1). For  $T \leq 160$  K the  $\alpha$ -peaks show a nonlinear increase below the peak frequency and consequently were fitted with the HN function, Eq. (3). Far below  $T_g^o$ , in the kHz–MHz region an additional relaxation process of rather low amplitude shows up, which was already noted in earlier dielectric studies.<sup>54,59</sup> For reasons given below, it will be denoted as  $\gamma$ -relaxation in the following. The relaxation peaks are shown in more detail in the inset of Fig. 9 also including fits with the CC function.

At 150–160 K, about 2 decades above  $\nu_p$ , deviations of experimental spectra and fits show up that have the signature of an excess wing.<sup>3,20,21</sup> This excess contribution cannot be explained by the  $\gamma$ -relaxation detected at lower temperatures. For example, at 150 K the loss peak caused by this relaxation

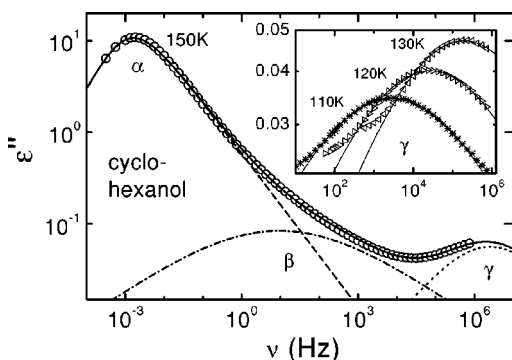


FIG. 9. Dielectric loss spectrum of cyclo-hexanol at 150 K. The solid line is a fit with the sum of a HN function (dashed line) and two CC functions (dash-dotted and dotted lines). The inset shows the region of the  $\gamma$ -relaxation at low temperatures. The lines are fits with the CC function.

process should be located at  $\nu > 1$  MHz (cf. inset of Fig. 9), which accounts for the increase of  $\varepsilon''(\nu)$  observed at  $\nu > 30$  kHz but not for the excess-wing feature. Following our recent findings for supercooled liquids, where the excess wing was revealed as the high-frequency flank of a  $\beta$ -relaxation peak, submerged under the dominating  $\alpha$ -peak,<sup>60</sup> we have fitted the spectrum at 150 K assuming an additive superposition of a HN function ( $\alpha$ -relaxation), a CC function ( $\beta$ -relaxation, causing the excess wing), and another CC function ( $\gamma$ -relaxation). As shown in Fig. 9, the experimental data can be perfectly described in this way. Of course, one should be aware that as long as the relaxations beyond the  $\alpha$ -relaxation do not show up as well-pronounced shoulders or even peaks in the spectrum, there is quite a lot of freedom in the choice of parameters. For example, in Fig. 9 the  $\beta$ -peak could be shifted to some extent towards lower frequencies, simultaneously increasing its amplitude, without considerably diminishing the quality of the fit. In the plastic phase, at temperatures  $T \geq 220$  K, deviations of measured spectra and fits show up that also resemble a (relatively weak) excess wing. For the highest frequencies (e.g., above about 100 MHz for 220 K), a stronger deviation is revealed that can be attributed to the  $\gamma$ -relaxation, shifted to frequencies above 100 MHz for these higher temperatures.

In Fig. 10 the relaxation times of the different processes in cyclo-hexanol are shown. The  $\alpha$ -relaxation times from the plastic phase match smoothly to those obtained in the supercooled plastic phase. As demonstrated by the solid and dashed lines,  $\tau_\alpha(T)$  can be described assuming a transition from a high-temperature Arrhenius- to a VFT-behavior at lower temperatures. Also a description with a second Arrhenius region with a higher energy barrier seems possible, however, leading to unreasonably low values of  $\tau_0$ . The  $\gamma$ -relaxation time behaves thermally activated. The points at 150 and 220 K ( $1000/T \approx 6.7$  and  $4.6 \text{ K}^{-1}$ , respectively) can only be rough estimates as, due to the limited frequency range, no actual loss-peaks are observed. The triangle in Fig. 10 represents the  $\beta$ -relaxation time obtained from the analysis shown in Fig. 9, again giving a rough estimate only. The present results agree reasonably with those reported in Refs. 55 and 59.<sup>61</sup> In the insets of Fig. 10 the high-frequency power-law exponent of the  $\alpha$ -peaks and the relaxation

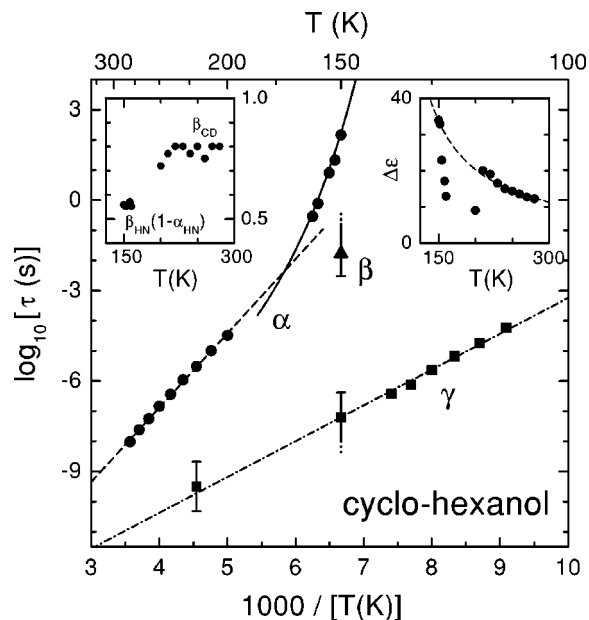


FIG. 10. Temperature dependence of the  $\alpha$ - and  $\gamma$ -relaxation time of cyclo-hexanol in Arrhenius representation. In addition the  $\beta$ -relaxation time at 150 K is given (triangle). The solid line shows a fit of  $\tau_\alpha(T)$  with the VFT law, Eq. (2), at  $T \leq 160$  K; the dashed line is an Arrhenius fit at  $T \geq 200$  K. The dash-dotted line is an Arrhenius fit of the  $\gamma$ -relaxation time. The left inset shows the power-law exponent of the high-frequency flanks of the  $\alpha$ -peaks as determined from the fits of the  $\alpha$ -peaks (Fig. 8). The right inset shows the relaxation strength  $\Delta\varepsilon$ ; the line demonstrates Curie-Weiss behavior for the temperatures that are not affected by a partial transition into the orientational state.

strength are given. Again both parameters determined in the plastic and supercooled plastic phases match smoothly together, except for  $\Delta\varepsilon(T)$  at  $154 \text{ K} \leq T \leq 200 \text{ K}$  where the peak amplitudes are diminished due to the successive transition into the orientationally ordered state. The low-frequency exponent  $\alpha_{\text{HN}}$  of the HN function, applied at  $T \leq 160$  K, varies between 0.15 and 0.35. These values are of somewhat restricted significance due to the limited frequency range available at  $\nu < \nu_p$ . While a Curie law does not lead to a reasonable fit of  $\Delta\varepsilon(T)$ , it can be parameterized with a Curie-Weiss behavior with  $T_C = 74 \text{ K}$  (dashed line in the right inset of Fig. 10). For  $\varepsilon_\infty$  a nearly temperature-independent value of 3.4 is obtained.

## E. Ethanol

As demonstrated first in the heat capacity measurements of Haida *et al.*<sup>62</sup> ethanol belongs to the few materials that can be prepared both in a supercooled liquid and a plastic phase. Aside from a number of dielectric investigations performed in structurally disordered ethanol,<sup>63–66</sup> recently extensive dielectric studies of the plastic crystalline phase of ethanol, including a comparison to the structurally disordered state, were reported.<sup>7,10,67,68</sup> In the present work we show spectra of ethanol in its supercooled plastic phase in an extended frequency range and analyze them in accordance with our interpretation of the dielectric spectra in the structurally disordered state of ethanol.<sup>66</sup>

To prepare ethanol in its plastic phase, a sample, previously quenched into the structurally disordered glass state,



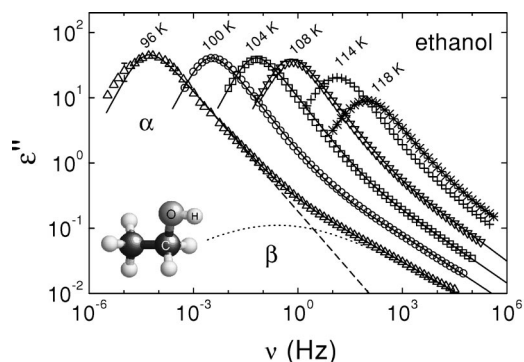


FIG. 11. Dielectric loss spectra of plastic-crystalline ethanol for various temperatures. The solid lines are fits with the sum of a CD and a CC function. For 96 K the two constituents of the fit are shown by the dashed and dotted line. The inset shows a schematic view of the molecular structure.

was slowly heated until at 106 K crystallization into the plastic crystalline state occurred. After subsequent cooling to 96 K, dielectric spectra were collected under heating, the results being shown in Fig. 11. Starting at about 108 K the transition into the completely ordered state sets in, leading to a reduction of the peak amplitudes above this temperature. Above about 120 K, spectra in the plastic phase of ethanol could not be collected as here always the completely ordered state is attained. In agreement with earlier reports,<sup>7,68</sup> the  $\alpha$ -peaks showing up in Fig. 11 exhibit a well-pronounced excess wing, very similar to the findings in structurally disordered ethanol,<sup>7,66,68</sup> shown in Fig. 12 for comparison.<sup>66</sup> For the latter, this excess wing develops into a shoulder for temperatures above 120 K (Fig. 12).<sup>66</sup> Obviously it is due to a  $\beta$ -relaxation, which at lower temperatures is submerged under the dominating  $\alpha$ -peak, only its high-frequency wing showing up in the spectra as an excess wing of the  $\alpha$ -peak. It seems natural to explain the excess wing in plastic-crystalline ethanol on the same footage, assuming that the  $\beta$ -relaxation process is in effect in both disordered phases. Indeed already in Ref. 68 the experimental spectra collected between 96 and 108 K were successfully fitted with a sum of two CD functions. Here we employ the sum of a CD and a CC function; as mentioned above,  $\beta$ -relaxations are known

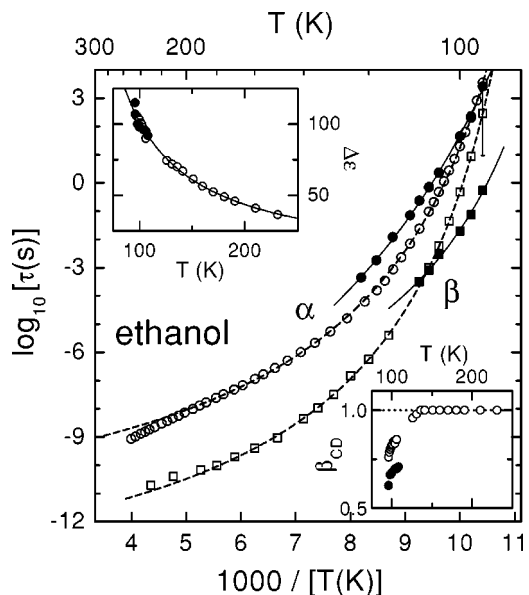


FIG. 13. Temperature dependence of the  $\alpha$ - and  $\beta$ -relaxation times of structurally (open symbols) (Ref. 66) and orientationally (closed symbols) disordered ethanol in Arrhenius representation. The lines are fits with the VFT law, Eq. (2). The lower inset shows  $\beta_{CD}$  of both disordered phases as determined from the fits of the  $\alpha$ -peaks (Figs. 11 and 12). The upper inset shows the relaxation strengths  $\Delta\epsilon$ , fitted with Curie-Weiss behavior.

to commonly follow a CC behavior. As shown by the solid lines in Fig. 11 this ansatz is able to describe the experimental data satisfactorily. In Fig. 13 the resulting relaxation times of the  $\alpha$ - and  $\beta$ -process are shown, together with those for structurally disordered ethanol.<sup>66</sup> In agreement with earlier reports,<sup>7,68</sup> for higher temperatures the  $\alpha$ -relaxation is significantly slower for the plastic phase, but approaches values nearly identical to those of the supercooled liquid for low temperatures. The latter behavior mirrors the identical glass temperatures of both disordered phases.<sup>62</sup> Similar to the supercooled liquid, however somewhat less pronounced,  $\tau_{\alpha}(T)$  deviates significantly from Arrhenius behavior and can be parameterized by the VFT function, Eq. (2) (solid line in Fig. 13, for parameters, see Table I). Also the  $\beta$ -relaxation time  $\tau_{\beta}$  of plastic crystalline ethanol (closed squares in Fig. 13) can be described by a VFT curve, as also found for the struc-

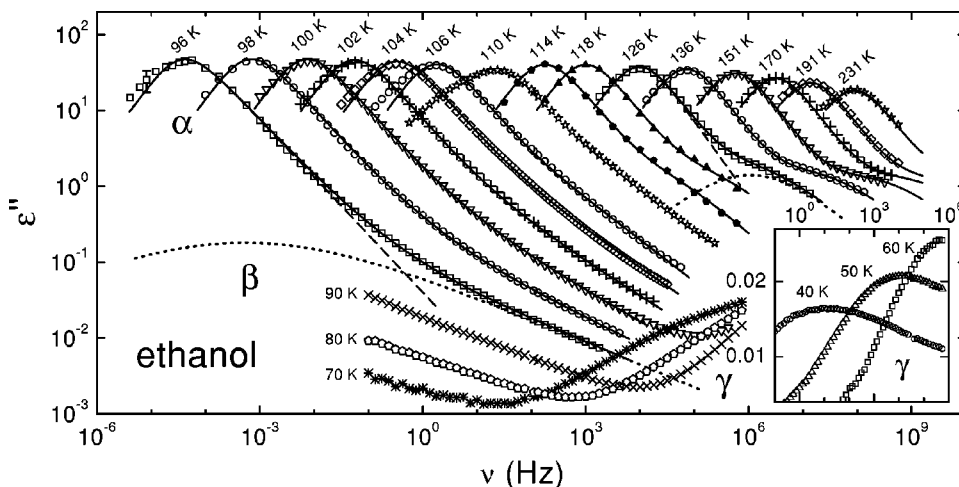


FIG. 12. Frequency-dependent dielectric loss of structurally disordered ethanol for various temperatures. The solid lines are fits with the sum of a CD and a CC function. For 86 K and 126 K, the dashed lines show the two constituents of the fits. The inset gives a separate view of the low-temperature results. [Reproduced from Ref. 66. Copyright (2000) by the American Physical Society.]



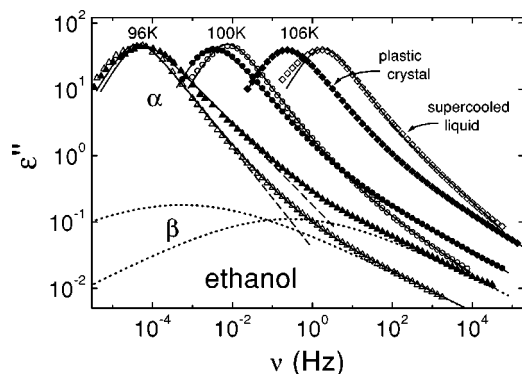


FIG. 14. Comparison of the dielectric loss spectra of structurally (open symbols) (Ref. 66) and orientationally (closed symbols) disordered ethanol. The solid lines are fits with the sum of a CD and a CC function. For 96 K the two constituents of the fits are shown by the dashed and dotted lines.

turally disordered phase (open squares in Fig. 13).<sup>66</sup> Within the scatter of the data, also an Arrhenius behavior seems possible, however leading to unreasonably low values of  $\tau_0$ .<sup>28</sup> The  $\beta$ -relaxation times of the two disordered phases show significantly different behavior. Of course one has to be aware of the very high uncertainty in the determination of this parameter, as only the high-frequency flank of the  $\beta$ -peak is visible in the spectra (cf. Fig. 11). However, that there is in fact a significant difference in the  $\beta$ -relaxation parameters is clearly revealed in Fig. 14 where the loss spectra for both disordered phases of ethanol are compared for three temperatures. For the plastic crystalline phase the excess wing caused by the  $\beta$ -relaxation is clearly stronger, most probably due to a smaller  $\tau_\beta$ , but also the amplitude and especially the width of the  $\beta$ -relaxations in the two phases may differ. In addition, the  $\alpha$ -peak is significantly broader for the plastic crystalline state, which, in agreement with earlier reports,<sup>7,68</sup> also shows up in a difference of  $\beta_{CD}(T)$  (lower inset of Fig. 13). The  $\alpha$ -relaxation strengths for both phases are shown in the left inset of Fig. 13, both agreeing reasonably. The line shows a parameterization with Curie-Weiss behavior ( $T_C=25$  K), a Curie law does not lead to reasonable fits.

Finally it should be mentioned that there is a further process that was detected at  $T < T_g^o$  in both disordered phases of ethanol<sup>7,10,66,68</sup> and denoted as  $\beta$ -process in Refs. 7 and 68. In Ref. 68 it was ascribed to local molecular librations, coupled to intramolecular motions. Extrapolating its relaxation time to temperatures above  $T_g^o$  leads to the conclusion that this process, which should be denoted as the  $\gamma$ -process in our interpretation, cannot be responsible for the observed excess wing, its peak being located at  $\nu > 100$  MHz for the relevant temperature region.

## F. Meta-carborane

The carborane molecule,  $B_{10}C_2H_{12}$ , forms an almost regularly shaped icosahedron whose corners are occupied by ten boron and two carbon atoms. The icosahedron is surrounded by 12 outward-bonded hydrogen atoms. For ortho-carborane the two carbon atoms occupy adjacent positions, for meta-carborane they are separated by one boron atom,

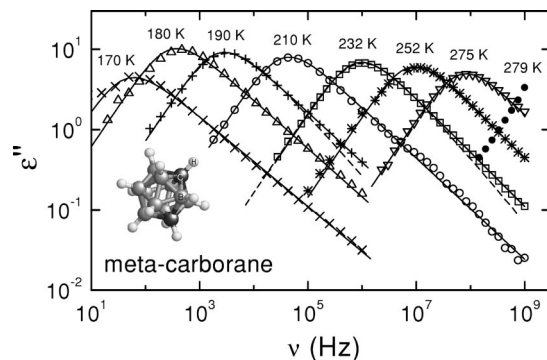


FIG. 15. Dielectric loss spectra of meta-carborane for various temperatures. The solid lines are fits with a CD function, Eq. (1). The inset shows a schematic view of the molecular structure.

and for para-carborane the carbon atoms are located at opposite sides of the icosahedron. The latter cannot be investigated dielectrically due to the lack of a dipolar moment. Overall, the carborane molecules are nearly spherically shaped and therefore experience little steric hindrance for reorientational processes, thus favoring the forming of a plastic-crystalline phase. Having a very rigid molecular structure, intramolecular excitations are expected at very high frequencies only and indeed were observed in mid- and near-infrared measurements above about 20 THz.<sup>28,69</sup> While detailed dielectric data are available for ortho-carborane,<sup>70</sup> for meta-carborane so far only dielectric spectra have been published without information on the parameters of the  $\alpha$ -relaxation.<sup>9</sup> At room temperature, the meta-carborane molecules undergo nearly free reorientations (Phase I),<sup>71-73</sup> but due to the strong sublimation tendency this state is difficult to investigate. Similar to ortho-carborane, somewhat below room temperature, meta-carborane undergoes a phase transition where the reorientational motion becomes partly restricted (phase II).<sup>72,74-76</sup> At a second transition near 170 K<sup>72,74</sup> finally complete orientational order is reached (phase III). As for adamantanone (Sec. III B) we believe that the restriction of motion in phase II of meta-carborane still allows the molecules to fully respond to the electrical field; some arguments for this notion concerning the similar phase transition in ortho-carborane are put forward in Ref. 70.

In Fig. 15 the loss spectra of meta-carborane are shown. In phase I, at 279 K the relaxation peak is located above the highest frequency investigated in this material and consequently only its low-frequency wing is visible. Assuming a constant amplitude and width and taking into account the real part, a peak position of about 3 GHz can be estimated. The restriction of the reorientation at the transition into phase II is accompanied by a slowing down of the dynamics. This behavior is similar to that found in adamantanone (Sec. III B), however, with a less dramatic slowing down of about a factor of 20. At 170 K the transition to the completely ordered phase III starts, leading to a reduced peak amplitude. As already emphasized in Ref. 9, the loss spectra of meta- and ortho-carborane show no indication of an excess wing or  $\beta$ -relaxation. The CD-function leads to almost perfect fits of the experimental data over up to eight frequency-decades (lines in Fig. 15).

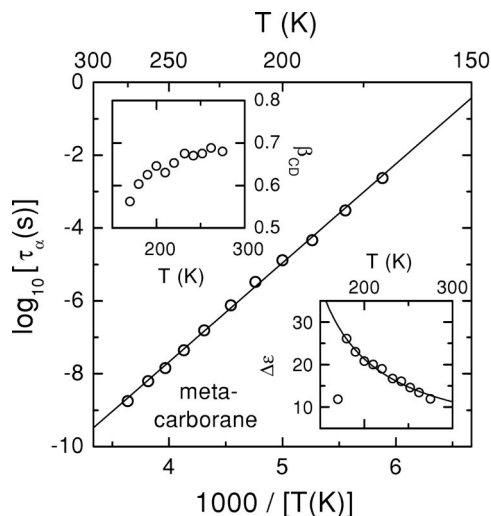


FIG. 16. Temperature dependence of the  $\alpha$ -relaxation time of meta-carborane in Arrhenius representation. The solid line shows a fit with Arrhenius behavior. The upper inset shows  $\beta_{CD}$  as determined from the fits of the  $\alpha$ -peaks (Fig. 15). The lower inset shows the relaxation strength  $\Delta\epsilon$ , fitted with a Curie-Weiss law (line).

It should be noted here that the Fourier transform of the KWW function leads to fits that show deviations from the experimental data at high frequencies<sup>77</sup> (dashed lines in Fig. 15), which could be mistaken as the indication of an excess wing. However, the spectra exhibit no indication of a second power law at  $\nu > \nu_p$ , which is the characteristic feature of an excess wing. As discussed in detail earlier,<sup>78</sup> in many cases, both for plastic crystals and supercooled liquids, in order to achieve a proper fit of the peak region with the Fourier transform of the KWW function, a value of  $\beta_{KWW}$  has to be chosen that is significantly higher than the exponent of the power law actually observed at  $\nu > \nu_p$ , consequently leading to an apparently stronger excess wing. As both, the CD and the KWW functions are essentially phenomenological descriptions only, there is no reason to prefer one or the other and in our experience in many cases the CD function leads to better fits of the experimental spectra.<sup>5,9,79–81</sup>

The parameters of the  $\alpha$ -relaxation are shown in Fig. 16. As for ortho-carborane,  $\tau_\alpha(T)$  follows Arrhenius behavior, the parameters being noted in Table I. The width parameter  $\beta_{CD}$  increases continuously with temperature and tends to saturate at a high-temperature value of about 0.7. The relaxation strength  $\Delta\epsilon$  increases towards low temperatures and can be parameterized by a Curie-Weiss law with  $T_C = 88$  K. In contrast, in ortho-carborane,  $\Delta\epsilon(T)$  increases towards low temperatures. This unusual behavior indicates cooperative motion of the molecules, most probably favored by the higher dipolar moment of the ortho-carborane molecule. For  $\epsilon_\infty$  a value of 3.2 is obtained.

## IV. DISCUSSION

### A. $\alpha$ -relaxation

As for most supercooled liquids, the  $\alpha$ -relaxation peaks in the investigated plastic-crystalline materials show marked deviations from a mono-dispersive Debye response being de-

scribable by the phenomenological CD or HN functions. In supercooled liquids, such a behavior is commonly ascribed to heterogeneity caused by the structural disorder leading to a distribution of relaxation times.<sup>82</sup> It is reasonable to assume that in plastic crystals the heterogeneity caused by orientational disorder leads to a distribution of relaxation times, too. Certainly intermolecular dipolar interactions play an important role here, but also steric hindrance may come into effect. With increasing temperature for the investigated plastic crystals the width of the  $\alpha$ -peaks is either constant or increases with temperature (often with a tendency to saturate at a value below unity) as also observed for most supercooled liquids. The relaxation strengths are either nearly constant or increase towards low temperatures, but in general do not follow a Curie law as would be expected from the Onsager theory.<sup>83</sup> Obviously in those cases  $\Delta\epsilon(T)$  cannot be understood easily and most probably strongly depends on details of the intermolecular interactions.

In 1-cyanoadamantane, cyclo-hexanol, and ethanol (Figs. 3, 10, and 13), all showing supercooled plastic-crystalline states, marked deviations of the temperature-dependent  $\alpha$ -relaxation time from Arrhenius behavior are revealed, as it is typical for most supercooled liquids, too. In a previous work,<sup>5</sup> we detected non-Arrhenius behavior also for supercooled plastic-crystalline cyclo-octanol. In the plastic crystals that show Arrhenius behavior of  $\tau_\alpha(T)$  in the whole temperature region investigated (Figs. 5, 7, and 16), the prefactors  $\tau_0$  (Table I) in general are lower than seems reasonable if one assumes that  $1/(2\pi\tau_0)$  should be of the order of a typical phonon frequency. Therefore deviations from Arrhenius behavior at higher (and possibly also lower) temperatures can be expected also for these materials. In 1-cyanoadamantane and cyclo-hexanol (Figs. 3 and 10), a transition from an Arrhenius at high temperatures to a Vogel-Fulcher temperature dependence at low temperatures is observed. A similar transition at a temperature  $T_A$  is found for some supercooled liquids, too<sup>63,78,84,85</sup> and is also revealed for supercooled-liquid ethanol in Fig. 13.<sup>66</sup>  $T_A$  was interpreted as temperature below which cooperativity sets in<sup>84</sup> or the potential energy landscape in configuration space becomes important,<sup>86</sup> both leading to deviations from simple thermally activated behavior.

The degree of deviation of  $\tau_\alpha(T)$  from thermally activated behavior provides a very useful classification of glass-forming materials.<sup>43</sup> Glass-formers are called “fragile” if their  $\tau_\alpha(T)$  curves deviate strongly from Arrhenius behavior and “strong” if  $\tau_\alpha(T)$  is nearly Arrhenius. The fragility classification has been connected to a microscopic picture by the assumption of different energy landscapes (i.e., potential energy versus configuration space) for strong and fragile liquids.<sup>87</sup> In order to obtain a quantitative measure of the “fragility,” the strength parameter  $D$  in Eq. (2) can be used.<sup>43</sup> As an alternative, the fragility parameter  $m$  was introduced,<sup>88,89</sup> which is defined by the slope at  $T_g$  in a plot of  $\log_{10}(\tau_\alpha)$  versus  $T_g/T$ , usually denoted as the Angell plot.<sup>90,91</sup> For strong systems  $m$  is near the minimum fragility parameter  $m_{\min} \approx 16$  while the most fragile glass formers have values of  $m$  up to 200.<sup>92</sup> For all plastic crystalline materials investigated in the present work, the orientational

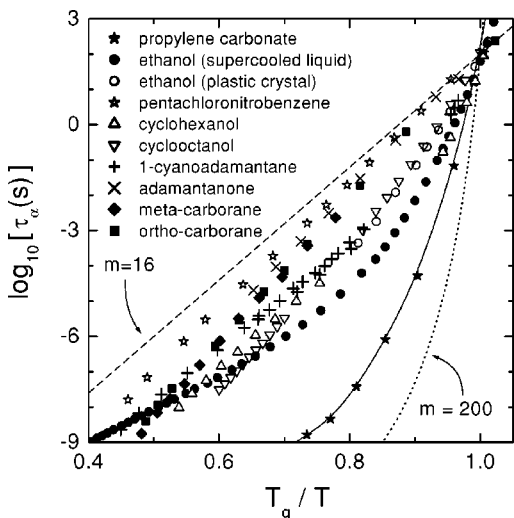


FIG. 17. Angell plot of the  $\alpha$ -relaxation times of the plastic-crystalline materials investigated in the present work, including also results on plastic-crystalline cyclo-octanol (Ref. 5) and ortho-carborane (Ref. 70). For comparison results on supercooled-liquid ethanol (Ref. 66) and propylene carbonate (Ref. 85) (the solid line is drawn to guide the eye) are shown. The dashed and dotted lines demonstrate the behavior for minimum and maximum fragility, respectively.

glass temperatures  $T_g^o$  as given in Table I were estimated from the  $\tau_\alpha(T)$  curves assuming  $\tau_\alpha(T_g^o) = 100$  s. Figure 17 shows the Angell plot for these materials; the fragility parameters deduced from the slope at  $T_g^o$  are given in Table I.<sup>93</sup> In addition, Fig. 17 includes the results for plastic crystalline cyclo-octanol ( $m = 33$ )<sup>5,94</sup> and ortho-carborane ( $m = 20$ )<sup>70</sup> measured in our group.<sup>5,70</sup> For comparison also the curves for a typical fragile structural glass former, propylene carbonate<sup>85</sup> ( $m = 104$ ) and for supercooled-liquid ethanol<sup>66</sup> ( $m = 48$ ) are given. Overall, all of the investigated plastic crystals can be characterized as strong or intermediate in the strong/fragile classification scheme. This finding agrees with the few cases where information on the fragility of plastic crystals is provided in literature.<sup>10,95–99</sup> The general tendency of the plastic crystalline state to be accompanied by a low fragility is nicely demonstrated in ethanol, where both structurally and orientationally disordered phases can be accessed. The missing structural disorder in plastic crystalline ethanol leads to a reduction of fragility from  $m = 48$  to 38 (cf. Table I). This behavior can be understood within the proposed connection of fragility and the potential energy landscape in configuration space.<sup>87</sup> Based on the inverse proportionality of effective energy barrier and configurational entropy deduced within the Adam–Gibbs theory,<sup>100</sup> the typical properties of fragile and strong glass formers can be rationalized assuming that the density of minima in the potential energy landscape increases with increasing fragility. For the plastic crystals the lattice symmetry can be presumed to lead to a reduced density of energy minima, which explains their relatively low fragility.

Interestingly, in Fig. 17 there seems to be the trend for molecules with high symmetry to exhibit the lowest fragilities. Especially the two carborane isomers and adamantanone with fragilities between 19 and 21 are very close to a globular molecular shape and the pentachloronitrobenzene mol-

ecule ( $m = 17$ ) comes close to a disk-like shape. There are also examples from literature: the ring-shaped thiopene<sup>95,96</sup> and the nearly spherical fullerene  $C_{60}$ ,<sup>97</sup> both with the smallest possible fragility of  $m = 16$ . It would be interesting to check for this trend also in the supercooled liquids, e.g., the glass formers with highest fragility are almost exclusively polymers.<sup>92</sup> But certainly other factors, as, e.g., the nature of the intermolecular bonds, play an important role here, too.

Yamamuro *et al.*<sup>98</sup> used a modified Adam–Gibbs theory in order to explain relaxation-time results on three plastic crystals. For isocyanocyclohexane and cyclo-hexanol, both of intermediate fragility, this theoretical approach worked well. However, for the strong 1-cyanoadamantane it had to be concluded that the Adam–Gibbs theory might not be applicable. In the Adam–Gibbs theory<sup>100</sup> the supercooled material is thought to be composed of cooperatively rearranging regions (CRRs). The number  $z$  of the molecules per region is assumed to increase as temperature decreases. This leads to a decrease of the configurational entropy and thereby an increase of the effective energy barrier for low temperatures, finally resulting in an expression for  $\tau_\alpha(T)$  virtually indistinguishable from the VFT equation. The results of Yamamuro *et al.*<sup>98</sup> suggest that the 1-cyanoadamantane molecules reorient essentially independently from each other, i.e.,  $z = 1$  and temperature independent, which leads to an Arrhenius behavior, thus explaining the low fragility. Possibly, the low fragility of the other highly symmetrical plastic crystals can be understood in a similar way. The low cooperativity of these materials then should be connected to their high symmetry, which possibly reduces intermolecular interactions via steric hindrance. But also the high molecular rigidity of those materials may play a role.<sup>98</sup>

## B. Excess wing and $\beta$ -relaxation

As we have seen in Sec. III, additional relaxation processes beyond the  $\alpha$ -process are quite common in plastic crystals.<sup>5,7,39,55,59</sup> Such additional relaxations, commonly termed  $\beta$ -,  $\gamma$ -relaxation, etc., are also observed in many other structural glass formers. In some cases these relaxations can be ascribed to an intramolecular dynamics, e.g., the movement of a molecular side-group in a polymer. But Johari and Goldstein demonstrated that additional relaxation processes also show up in glass formers, where intramolecular contributions seem unlikely and that these so-called Johari–Goldstein  $\beta$ -relaxations therefore may be inherent to glass-forming materials in general.<sup>101</sup> However, the microscopic process behind this kind of  $\beta$ -relaxations is still controversially discussed.

In some structural glass formers at frequencies several decades above  $\nu_p$  the empirical functions used for the description of the  $\alpha$ -peak fail and an “excess wing” shows up.<sup>3,10,20–23</sup> It can be reasonably well described<sup>21–23</sup> by a second power law,  $\epsilon'' \sim \nu^{-b}$  with  $b < \beta$  in addition to the power law  $\nu^{-\beta}$ , commonly found at  $\nu > \nu_p$ . A very interesting property of the excess wing was found by Nagel and coworkers:<sup>20</sup> By an appropriate scaling of the axes, it is possible to collapse the  $\epsilon''(\nu)$  curves, including the excess wing, for different temperatures and even for different materials onto one master curve. The applicability of this so-called



Nagel scaling has been controversially discussed during recent years<sup>9,102–104</sup> and many efforts have been made to check for its validity in a variety of materials.<sup>4,9,103,104</sup> Until recently it was commonly assumed that the excess wing and the Johari–Goldstein  $\beta$ -relaxations are due to different processes. However, it also seems possible that excess wing and  $\beta$ -relaxation are due to the same microscopic process as considered in several publications.<sup>21,78,105</sup> Indeed recently some strong experimental hints have emerged that the excess wing is simply the high-frequency flank of a  $\beta$ -peak, hidden under the dominating  $\alpha$ -peak.<sup>60</sup>

At this point some remarks on nomenclature may be helpful. The terms “ $\beta$ -relaxation,” “secondary relaxation,” and “Johari–Goldstein relaxation” often are used also to imply a specific experimental behavior or microscopic explanation of the observed relaxation process. For example, an Arrhenius temperature-dependence of the relaxation time is commonly assumed to be a typical signature of  $\beta$ - and JG-relaxations, and many people would be reluctant to designate relaxations with non-Arrhenius relaxation-time behavior as  $\beta$ - or JG-relaxations. However, within the recently emerging picture of an additional relaxation causing the excess wing, observed in some materials, it was proposed that this “excess-wing relaxation” is in fact a JG- $\beta$ -relaxation with an uncommon non-Arrhenius temperature dependence of the relaxation time.<sup>60</sup> To avoid confusion we suggest the following: All relaxation processes should be denoted by the Greek letters  $\alpha$ ,  $\beta$ ,  $\gamma$ , etc., in the succession of their appearance in the experimental spectra. Secondary relaxations are relaxations with reduced amplitude at frequencies beyond the  $\alpha$ -process. If the excess wing is identified to be due to a secondary relaxation process this process should be denoted as  $\beta$ -relaxation, irrespective of the temperature dependence of  $\tau_\beta$ . As the microscopic origin of  $\beta$ - or JG-relaxations is not yet clarified, there is no theoretical reason to restrict the term  $\beta$ -relaxation to processes with Arrhenius-like  $\tau_\beta(T)$ . The term JG-relaxation denotes secondary relaxations that do not have an intramolecular origin as, e.g., motions of a side group in a polymer. In their pioneering work, Johari and Goldstein<sup>101</sup> demonstrated that there are such  $\beta$ -relaxations that are not due to internal modes of the molecules but seem to be of more intrinsic origin and probably inherent to the glass-forming state. Also for JG processes a non-Arrhenius  $\tau_\beta(T)$  should not be excluded; already Johari and Goldstein speculated that there might be JG-relaxations with a “somewhat different frequency-temperature relationship” explaining the cases where the  $\beta$ -relaxation “has not been resolved from the main relaxation.”<sup>101</sup>

There are only a few claims of the observation of an excess wing in plastic crystals so far<sup>4,7,68,94</sup> and it was proposed that this feature may be generally absent in this class of disordered materials.<sup>9</sup> In the following, we want to check the present results for the occurrence of an excess wing. In Ref. 9 results on ortho- and meta-carborane isomers and on 1-cyanoadamantane were presented. As shown in Fig. 15, indeed in meta-carborane the spectra can be perfectly fitted with a CD function up to the highest frequencies. This is also the case for ortho-carborane.<sup>9</sup> In Fig. 2 spectra for 1-cyanoadamantane in an extended frequency and tempera-

ture range, compared to Ref. 9, are provided. The slight deviations of CD fits and experimental data partly can be ascribed to a  $\beta$ -relaxation detected at  $T < T_g^o$ .<sup>39</sup> This is demonstrated by the  $\beta$ -peak positions obtained from an extrapolation of  $\tau_\beta(T)$  of Ref. 39 up to high temperatures, which are indicated by arrows in Fig. 2. However, for the two highest temperatures shown, the  $\beta$ -relaxation cannot be responsible for the observed deviations from the CD curves. At these very high frequencies above 10 GHz, most probably  $\varepsilon''(\nu)$  already approaches the minimum that must exist between the  $\alpha$ -relaxation and the infrared excitations in the THz region. Indeed the presence of such a minimum was recently demonstrated not only for supercooled liquids<sup>3,106</sup> but also for two plastic crystals.<sup>5,24,107,108</sup> Concerning phase II of adamantanone (Fig. 4) and pentachloronitrobenzene (Fig. 6), as noted in Secs. III B and III C, the deviations of the loss spectra from the HN function are due to  $\beta$ -processes. The corresponding  $\beta$ -peaks are clearly revealed in the spectra at the lowest temperatures (Figs. 4 and 6), but submerged under the dominating  $\alpha$ -peaks at higher temperatures. The slight deviations seen in phase I of adamantanone (Fig. 4) again can be ascribed to the approach of the high-frequency minimum in  $\varepsilon''(\nu)$ . In cyclo-hexanol the situation is more complicated (Fig. 8): The excess-wing-like deviations cannot be ascribed to the relaxation seen at low temperatures and denoted as  $\gamma$ -relaxation. While a description of the excess wing, assuming a  $\beta$ -relaxation, is possible as demonstrated in Fig. 9, one has to state that this material is the only plastic crystal investigated by us until now, where we did not find clear evidence against an excess wing in its original sense, i.e., a second high-frequency power law that is part of the  $\alpha$ -relaxation and not connected with an additional relaxation. In ethanol (Figs. 11 and 12) the situation is clear: In Ref. 66 we found evidence for a  $\beta$ -relaxation as the origin of the apparent wing in the supercooled-liquid state of ethanol. Making the reasonable assumption that this  $\beta$ -relaxation is also present in the plastic phase, it explains the excess-wing-like deviations seen in the spectra.<sup>7,68</sup> Overall, except for cyclo-hexanol, in all plastic crystals investigated so far there is compelling evidence against the presence of an excess wing in its original sense.

In Fig. 18 spectra of all plastic crystals investigated, including cyclo-octanol<sup>5,108</sup> and ortho-carborane,<sup>9,70</sup> are shown in the scaling representation proposed by Nagel and coworkers.<sup>20</sup> For clarity reasons, a curve at one temperature only is shown for each material. For comparison, a curve for supercooled liquid propylene carbonate<sup>85,104</sup> is included, known to closely follow the master curve of Nagel and coworkers<sup>20</sup> at least in the frequency region relevant here.<sup>104</sup> Clearly the spectra of the investigated plastic crystals cannot be scaled in this way and in most cases the master curve is not matched. Also most of the scaled curves fall below the master curve. This finding is of special significance as spectra falling above the master curve can always be explained by contributions in addition to the excess wing (e.g., a  $\beta$ -relaxation), but this is not the case for spectra falling below the master curve. The Nagel scaling is clearly violated in plastic crystals.

Concerning the additional relaxation processes ( $\beta$ -,  $\gamma$ -)



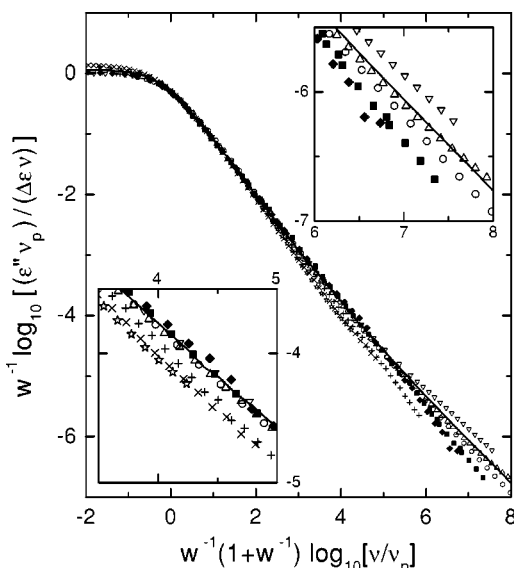


FIG. 18. Nagel-scaling plot (Ref. 20) for the plastic-crystalline materials investigated in the present work and plastic-crystalline cyclo-octanol (Ref. 5) and ortho-carborane (Refs. 9 and 70). For clarity reasons, spectra for only one temperature per material are given, namely: ethanol at 100 K (circles), pentachloronitrobenzene at 230 K (stars), cyclo-hexanol at 150 K (triangles up), cyclo-octanol at 200 K (triangles down), 1-cyanoadamantane at 300 K (pluses), adamantanone at 180 K ( $\times$ ), meta-carborane at 200 K (lozenges), ortho-carborane at 120 K (squares). For comparison also results for supercooled-liquid propylene carbonate (Ref. 85) at 158 K are included (line), which closely follow the master curve promoted in Ref. 20. The insets give magnified views of the middle and high-frequency sections.

observed in some of the investigated materials, in most cases one can only speculate about their origin. At least for the rigid adamantanone and cyanoadamantane molecules it can be excluded that the observed  $\beta$ -relaxations are due to intramolecular degrees of freedom. Instead more fundamental reasons for their appearance can be assumed, thus assuring that at least in these materials true Johari–Goldstein  $\beta$ -relaxations<sup>101</sup> are present. Also the results in supercooled and plastic-crystalline ethanol give some indication for a nonintramolecular origin of the  $\beta$ -relaxation causing the excess wing: While  $\tau_\alpha$  near the glass temperature is nearly identical for both disordered phases, the  $\beta$ -relaxation times differ by at least a decade (Figs. 13 and 14). It seems unlikely for an intramolecular motion to change its properties in dependence of the long-range translational order and thus we propose that the  $\beta$ -relaxation causing the excess wing in ethanol is of JG type. In contrast, the  $\gamma$ -relaxations, observed in supercooled and plastic crystalline ethanol (denoted as  $\beta$ -relaxations in Refs. 7 and 68) are very similar concerning relaxation time and other properties, suggesting an intramolecular origin.<sup>7,10,68</sup> Tentatively we also propose an intramolecular origin for the  $\gamma$ -relaxation observed in cyclohexanol (Sec. III D) and cyclo-octanol,<sup>5</sup> probably related with the presence of the OH-group in those plastic-crystalline alcohols.

Recently for glass formers with a well-pronounced  $\beta$ -relaxation, a correlation of  $\tau_\beta$  and the Kohlrausch exponent  $\beta_{\text{KWW}}$ , both at  $T'_g$ , was found:<sup>109</sup>  $\log_{10} \tau_\beta(T'_g)$  increases nearly linearly with  $\beta_{\text{KWW}}(T'_g)$ . Here  $T'_g$  was defined as the temperature where  $\tau_\alpha = 10^4$  s. It was noted that those

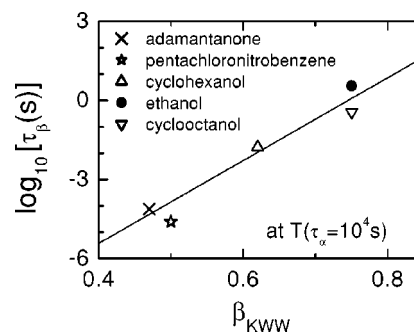


FIG. 19.  $\beta$ -relaxation time vs  $\alpha$ -relaxation width-parameter  $\beta_{\text{KWW}}$  for five plastic-crystalline materials (data on cyclo-octanol from Ref. 5). Both parameters were taken at  $T'_g$ , defined as the temperature where  $\tau_\alpha = 10^4$  s. The line shows the prediction of the coupling model (Ref. 109).

glass formers that show an excess wing instead of a clearly resolved  $\beta$ -relaxation have relatively large values of  $\beta_{\text{KWW}}(T'_g)$ . As the mentioned correlation implies that the  $\alpha$ - and  $\beta$ -time scales approach each other with increasing  $\beta_{\text{KWW}}(T'_g)$ , it is easily rationalized that in those materials the  $\beta$ -relaxation does not show up as a separate peak or shoulder. In Fig. 19 those plastic crystals investigated in the present work that show a  $\beta$ -relaxation are checked for the validity of the correlation proposed in Ref. 109.<sup>110</sup> In addition a point for cyclo-octanol is included, determined from the data in Ref. 5. Despite some uncertainty in the determination, especially of  $\tau_\beta(T'_g)$ , and the necessary extrapolations to low temperatures, this correlation seems to be rather well fulfilled also for plastic crystals. In Ref. 109 an explanation of this correlation within the coupling model<sup>111</sup> was proposed. The line in Fig. 19 shows the theoretical prediction for the “primitive  $\alpha$ -relaxation time” of the coupling model, which is assumed to be of similar magnitude as  $\tau_\beta$ .<sup>109</sup> Also the difference in  $\tau_\beta$  for supercooled-liquid and plastic-crystalline ethanol at 96 K ( $\approx T'_g$ ) can be traced back to the difference in the  $\alpha$ -peak width within this scheme (Figs. 13 and 14).

## V. CONCLUSIONS

In the present work the dielectric response of six plastic-crystalline materials has been investigated. A variety of new information on the relaxational behavior of the different materials has been collected, e.g., the presence of dipolar-active reorientational motion in phase II of adamantanone and of  $\beta$ -relaxations in pentachloronitrobenzene and adamantanone. In general, concerning the  $\alpha$ -relaxation the investigated plastic crystals exhibit the typical characteristics known from the structurally disordered supercooled liquids, e.g., nonexponential relaxation and various degrees of deviations of  $\tau_\alpha(T)$  from Arrhenius behavior. Generally, plastic crystals are strong or intermediate “glass” formers in Angell’s classification scheme.<sup>43</sup> Most likely, the presence of lattice symmetry leads to a reduced density of energy minima of the energy landscape in configuration space,<sup>87</sup> if compared to structurally disordered materials. In addition, our results and those in literature reveal a tendency for the systems with the most symmetrical molecules to exhibit the lowest fragilities. This

finding seems to be in accord with the earlier result of low cooperativity in 1-cyanoadamantane, which is based on a modified Adam–Gibbs theory.<sup>98</sup>

But there is one significant difference of the  $\alpha$  response in plastic crystals when compared to canonical supercooled liquids. In most glass formers the low-frequency wing of the structural relaxation peaks follows almost a Debye behavior. This is certainly not the case in plastic crystals. In many of the plastic crystals and specifically those undergoing a order–disorder phase transition, the  $\alpha$ -response in the low-temperature phase, where the molecules undergo a hindered rotation only, show a low-frequency slope which is significantly lower than one in a double-logarithmic representation. At low temperatures, in pentachloronitrobenzene or in adamantanone, the slope reaches values of almost 0.5. This means that in addition to the characteristic asymmetric shape of the  $\alpha$ -response in supercooled liquids, in plastic crystals it is symmetrically broadened, which results from the fact that the molecules reorient in potentials whose barriers are distributed and effectively frozen in. Assuming a fixed Gaussian distribution of energy barriers will yield a symmetric  $1/T$  broadening of the  $\alpha$ -response in a double logarithmic plot.<sup>18</sup> Hence plastic crystals, in addition to cooperativity, always reveal the presence of random fields, which broaden the relaxation processes symmetrically.

In most of the investigated plastic crystals,  $\beta$ -relaxations were detected. From our results an intramolecular origin of these relaxations seems unlikely, i.e., those relaxations can be assumed to be of the Johari–Goldstein type.<sup>101</sup> The recently found correlation of  $\alpha$ -peak width and  $\beta$ -relaxation time<sup>109</sup> seems to be fulfilled in plastic crystals, which also points to a more fundamental origin of the  $\beta$ -relaxation. However, the microscopic processes behind this kind of  $\beta$ -relaxations are still controversially discussed (see, e.g., Ref. 23).

In Ref. 9, the notion was promoted that in plastic crystals there is no excess wing, i.e., an additional high-frequency power law, which is part of the  $\alpha$ -relaxation. This notion is fully corroborated by the present results. Either the excess wing is completely absent (in meta- and ortho-carborane<sup>9</sup>) or an apparent excess wing shows up, that, however, can be ascribed to an underlying  $\beta$ -relaxation (in 1-cyanoadamantane, adamantanone, pentachloronitrobenzene, ethanol, and cyclo-octanol<sup>5</sup>). For cyclo-hexanol a clear statement is not possible, but at least the data are consistent with the above scenario. Very recently, experimental evidence was found that even in supercooled liquids there may be no excess wing in its original sense: Also here it may always be ascribable to a  $\beta$ -relaxation peak, submerged under the  $\alpha$ -peak.<sup>60</sup> Therefore the question risen by the present results should not be: “Why is the excess wing absent in plastic crystals?” but “Why in some plastic crystals (e.g., the carboranes), is the  $\beta$ -relaxation so weak or even absent that no apparent excess wing emerges and why in others (e.g., ethanol) is the  $\beta$ -relaxation of similar magnitude as in supercooled liquids?” Another important question concerns the Nagel scaling which fails in plastic crystals, but seems to work quite well in supercooled liquids. The Nagel scaling implies a close connection of the parameters of the  $\alpha$ - and

the  $\beta$ -relaxation, which only partly has been explained in terms of the mentioned relation of  $\beta_{\text{KWW}}$  and  $\tau_{\alpha}$ .<sup>109</sup> Obviously in supercooled liquids also a relation must exist between the amplitudes of both processes, which, however, is not valid in the plastic crystals. From the present results it seems that in general the amplitude of the  $\beta$ -relaxation is weaker in plastic crystals than in supercooled liquids. Obviously the  $\beta$ -relaxation must be favored in some way by the presence of structural disorder. All these open questions certainly are difficult to answer and would require a thorough understanding of the origin of the  $\beta$ -relaxation. At least, if the picture of a  $\beta$ -relaxation causing the excess wing is correct, one has to look for an explanation of one phenomenon only ( $\beta$ -relaxation), instead of two separate ones (excess wing and  $\beta$ -relaxation).

## ACKNOWLEDGMENTS

The authors gratefully acknowledge stimulating discussions with K. L. Ngai. This work was supported by the Deutsche Forschungsgemeinschaft, Grant Nos. LO264/8-1 and LO264/9-1.

<sup>1</sup>P. W. Anderson, *Science* **267**, 1615 (1995).

<sup>2</sup>For some recent reviews on the physics of glass-forming materials, see: M. D. Ediger, C. A. Angell, and S. R. Nagel, *J. Phys. Chem.* **100**, 13200 (1996); K. L. Ngai, *J. Non-Cryst. Solids* **275**, 7 (2000); C. A. Angell, K. L. Ngai, G. B. McKenna, P. F. McMillan, and S. W. Martin, *J. Appl. Phys.* **88**, 3113 (2000).

<sup>3</sup>P. Lunkenheimer, U. Schneider, R. Brand, and A. Loidl, *Contemp. Phys.* **41**, 15 (2000).

<sup>4</sup>D. L. Leslie-Pelecky and N. O. Birge, *Phys. Rev. Lett.* **72**, 1232 (1994).

<sup>5</sup>R. Brand, P. Lunkenheimer, and A. Loidl, *Phys. Rev. B* **56**, R5713 (1997).

<sup>6</sup>B. Kuchta, M. Descamps, and F. Affouard, *J. Chem. Phys.* **109**, 6753 (1998).

<sup>7</sup>S. Benkhof, A. Kudlik, T. Blochowicz, and E. Rössler, *J. Phys.: Condens. Matter* **10**, 8155 (1998).

<sup>8</sup>M. Jiménez-Ruiz, A. Criado, F. J. Bermejo, G. J. Cuello, F. R. Trouw, R. Fernández-Perea, H. Löwen, C. Cabrillo, and H. E. Fischer, *Phys. Rev. Lett.* **83**, 2757 (1999).

<sup>9</sup>R. Brand, P. Lunkenheimer, U. Schneider, and A. Loidl, *Phys. Rev. Lett.* **82**, 1951 (1999).

<sup>10</sup>S. Benkhof, T. Blochowicz, A. Kudlik, C. Tschirwitz, and E. Rössler, *Ferroelectrics* **236**, 193 (2000).

<sup>11</sup>R. Böhmer, G. Diezemann, G. Hinze, and E. Rössler, *Prog. Nucl. Magn. Reson. Spectrosc.* **39**, 191 (2001).

<sup>12</sup>F. Simon and C. von Simson, *Z. Phys.* **21**, 168 (1924).

<sup>13</sup>J. Timmermans, *J. Chim. Phys.* **35**, 331 (1938).

<sup>14</sup>P. A. Winsor, in *Liquid Crystals and Plastic Crystals*, Vol. 1, edited by G. W. Gray and P. A. Winsor (Wiley, New York, 1974), p. 48.

<sup>15</sup>N. G. Parsonage and L. A. K. Staveley, *Disorder in Crystals* (Oxford University, Oxford, 1978).

<sup>16</sup>J. N. Sherwood, *The Plastically Crystalline State* (Wiley, New York, 1979).

<sup>17</sup>K. Adachi, H. Suga, and S. Seki, *Bull. Chem. Soc. Jpn.* **41**, 1073 (1968).

<sup>18</sup>U. T. Höchli, K. Knorr, and A. Loidl, *Adv. Phys.* **39**, 405 (1990); A. Loidl and R. Böhmer, in *Disorder Effects on Relaxational Processes*, edited by R. Richert and A. Blumen (Springer, Berlin, 1994), p. 659.

<sup>19</sup>A. Srinivasan, F. J. Bermejo, A. de Andrés, J. Dawidowski, J. Zúñiga, and A. Criado, *Phys. Rev. B* **53**, 8172 (1996); M. A. Ramos, S. Vieira, F. J. Bermejo, J. Dawidowski, H. E. Fischer, H. Schober, M. A. González, C. K. Loong, and D. L. Price, *Phys. Rev. Lett.* **78**, 82 (1997); M. A. Miller, J. Ruiz, F. J. Bermejo, and N. O. Birge, *Phys. Rev. B* **57**, R13977 (1998).

<sup>20</sup>P. K. Dixon, L. Wu, S. R. Nagel, B. D. Williams, and J. P. Carini, *Phys. Rev. Lett.* **65**, 1108 (1990).

<sup>21</sup>A. Hofmann, F. Kremer, E. W. Fischer, and A. Schönhals, in *Disorder Effects on Relaxational Processes*, edited by R. Richert and A. Blumen (Springer, Berlin, 1994), p. 309.

- <sup>22</sup>R. L. Leheny and S. R. Nagel, *Europhys. Lett.* **39**, 447 (1997).
- <sup>23</sup>A. Kudlik, S. Benkhof, T. Blochowicz, C. Tschirwitz, and E. Rössler, *J. Mol. Struct.* **479**, 201 (1999).
- <sup>24</sup>P. Lunkenheimer, R. Brand, and A. Loidl (unpublished).
- <sup>25</sup>R. Böhmer, B. Schiener, J. Hemberger, and R. V. Chamberlin, *Z. Phys.* **99**, 91 (1995).
- <sup>26</sup>R. Böhmer, M. Maglione, P. Lunkenheimer, and A. Loidl, *J. Appl. Phys.* **65**, 901 (1989).
- <sup>27</sup>U. Schneider, P. Lunkenheimer, A. Pimenov, R. Brand, and A. Loidl, *Ferroelectrics* **249**, 89 (2001).
- <sup>28</sup>R. Brand, *Breitbandige dielektrische Spektroskopie zur Untersuchung der Glasdynamik plastischer Kristalle* (Pro Business, Berlin, 2001).
- <sup>29</sup>S. Havriliak and S. Negami, *J. Polym. Sci., Part C: Polym. Symp.* **14**, 99 (1966).
- <sup>30</sup>K. S. Cole and R. H. Cole, *J. Chem. Phys.* **9**, 341 (1941).
- <sup>31</sup>D. W. Davidson and R. H. Cole, *J. Chem. Phys.* **18**, 1417 (1950); **19**, 1484 (1951).
- <sup>32</sup>H. Vogel, *Phys. Z.* **22**, 645 (1921); G. S. Fulcher, *J. Am. Ceram. Soc.* **8**, 339 (1923); G. Tammann and W. Hesse, *Z. Anorg. Allg. Chem.* **156**, 245 (1926).
- <sup>33</sup>J. L. Sauvajol, M. Bée, and J. P. Amoureux, *Mol. Phys.* **46**, 811 (1982).
- <sup>34</sup>J. P. Amoureux and M. Bée, *Acta Crystallogr., Sect. B: Struct. Crystallogr. Cryst. Chem.* **35**, 2957 (1979); J. L. Sauvajol, M. Bée, and J. P. Amoureux, *Mol. Phys.* **46**, 811 (1982); J. P. Amoureux, R. Decressain, M. Sahour, and E. Cochon, *J. Phys. II* **2**, 249 (1992); M. Descamps, J. F. Willart, B. Kuchta, and F. Affouard, *J. Non-Cryst. Solids* **235–237**, 559 (1998).
- <sup>35</sup>M. Foulon, J. P. Amoureux, J. L. Sauvajol, J. P. Cavrot, and M. Muller, *J. Phys. C* **17**, 4213 (1984).
- <sup>36</sup>M. Descamps, J. F. Willart, and O. Delcourt, *Physica A* **201**, 346 (1993).
- <sup>37</sup>J. P. Amoureux, M. Castelein, M. D. Benadda, M. Bée, and J. L. Sauvajol, *J. Phys. (France)* **44**, 513 (1983).
- <sup>38</sup>J. P. Amoureux, G. Noyel, M. Foulon, M. Bée, and L. Jorat, *Mol. Phys.* **52**, 161 (1984).
- <sup>39</sup>K. Pathmanathan and G. P. Johari, *J. Phys. C* **18**, 6535 (1985).
- <sup>40</sup>M. Tyagi and S. S. N. Murthy, *J. Chem. Phys.* **114**, 3640 (2001).
- <sup>41</sup>R. Kohlrausch, *Ann. Phys. (Leipzig)* **167**, 179 (1854); G. Williams and D. C. Watts, *Trans. Faraday Soc.* **66**, 80 (1970).
- <sup>42</sup>Here and in the following, as not all spectra were actually fitted,  $\tau_\alpha$  partly was determined from the peak frequency ( $1/\tau_\alpha \approx \nu_p$ ). The difference to  $\tau_\alpha$  determined from the fits is only marginal. Concerning the fit results, for the CD function  $\tau_\alpha$  represents the average relaxation time  $\langle \tau_\alpha \rangle = \tau_{CD} \tau_{BCD}$ . For the HN function  $\langle \tau_\alpha \rangle$  is not defined and  $\tau_\alpha = \tau_{HN}$  is used as an estimate of  $\langle \tau_\alpha \rangle$ .
- <sup>43</sup>C. A. Angell, in *Relaxations in Complex Systems*, edited by K. L. Ngai and G. B. Wright (NRL, Washington, DC, 1985), p. 3.
- <sup>44</sup>J. P. Amoureux, M. Castelein, M. Bée, B. Arnaud, and M. L. Shouteeten, *J. Phys. C* **15**, 1319 (1982); R. Decressain, J. P. Amoureux, and E. Cochon, *Phys. Status Solidi B* **190**, 295 (1995).
- <sup>45</sup>J. P. Amoureux, M. Sahour, C. Fernandez, and P. Bodart, *Phys. Status Solidi A* **143**, 441 (1994).
- <sup>46</sup>J. P. Amoureux and M. Bée, *J. Phys. C* **13**, 3577 (1980); M. Bée, J. P. Amoureux, and J. Dianoux, *Mol. Phys.* **41**, 325 (1980).
- <sup>47</sup>In the course of the present paper, if multiple peaks show up in the spectra, they are denoted as  $\alpha$ -,  $\beta$ -, etc., according to the succession of their appearance in the frequency range. This denotation does not imply any physical interpretation or specific behavior, sometimes associated with the term  $\beta$ -relaxation (see Sec. IV B for a more detailed discussion).
- <sup>48</sup>The justification for using an additive superposition of different contributions to the susceptibility is controversially discussed [e.g., E. Donth, K. Schröter, and S. Kahle, *Phys. Rev. E* **60**, 1099 (1999); A. Arbe, J. Colmenero, D. Gómez, D. Richter, and B. Farago, *ibid.* **60**, 1103 (1999)], but nevertheless seems sufficient for a first analysis. It certainly is a good approximation if the time scales of both processes are well separated, which is fulfilled in most of the cases considered in the present work.
- <sup>49</sup>R. Böhmer, *J. Chem. Phys.* **91**, 3111 (1989); L. Wu, *Phys. Rev. B* **43**, 9906 (1991).
- <sup>50</sup>A. Aihara, C. Kitazawa, and A. Nohara, *Bull. Chem. Soc. Jpn.* **43**, 3750 (1970).
- <sup>51</sup>P. G. Hall and G. S. Horsfall, *J. Chem. Soc., Faraday Trans. 2* **69**, 1071 (1974).
- <sup>52</sup>H. A. Kolodziej, K. Orzechowski, R. Szostak, P. Freundlich, T. Głowiak, and S. Sorriso, *J. Mol. Struct.* **380**, 15 (1995).
- <sup>53</sup>For example, T. Matsuo, H. Suga, and S. Seki, *Bull. Chem. Soc. Jpn.* **39**, 1837 (1966); K. Kishimoto, H. Suga, and S. Seki, *ibid.* **53**, 2748 (1980); A. Dworkin, A. H. Fuchs, M. Ghelfenstein, and H. Szwarc, *J. Phys. (France)* **43**, L21 (1982); S. Stapf and R. Kimmich, *Mol. Phys.* **92**, 1051 (1997).
- <sup>54</sup>P. L. Kuhns and M. S. Conradi, *J. Chem. Phys.* **80**, 5851 (1984).
- <sup>55</sup>K. Adachi, H. Suga, S. Seki, S. Kubota, S. Yamaguchi, O. Yano, and Y. Wada, *Mol. Cryst. Liq. Cryst.* **18**, 345 (1972).
- <sup>56</sup>M. Shablakh, L. A. Dissado, and R. M. Hill, *J. Chem. Soc., Faraday Trans. 2* **79**, 369 (1983).
- <sup>57</sup>T. Shinomiya, *Bull. Chem. Soc. Jpn.* **63**, 1087 (1990).
- <sup>58</sup>M. Stockhausen and S. von Hornhardt, *Z. Naturforsch., A: Phys. Sci.* **47**, 1135 (1992).
- <sup>59</sup>Gangasharan and S. S. N. Murthy, *J. Chem. Phys.* **99**, 9865 (1993).
- <sup>60</sup>U. Schneider, R. Brand, P. Lunkenheimer, and A. Loidl, *Phys. Rev. Lett.* **84**, 5560 (2000).
- <sup>61</sup>The  $\gamma$ -relaxation times, deduced from the peak positions of the loss spectra shown in Fig. 12 of Ref. 55, agree with the present results, while those deduced from Fig. 11 of Ref. 55 (peak position vs inverse temperature) differ from those reported here by about one decade.
- <sup>62</sup>O. Haida, H. Suga, and S. Seki, *Proc. Jpn. Acad.* **48**, 683 (1972); O. Haida, H. Suga, and S. Seki, *J. Chem. Thermodyn.* **9**, 1133 (1977).
- <sup>63</sup>F. Stickel, E. W. Fischer, and R. Richert, *J. Chem. Phys.* **104**, 2043 (1996).
- <sup>64</sup>F. X. Hassion and R. H. Cole, *J. Chem. Phys.* **23**, 1756 (1955).
- <sup>65</sup>J. Barthel, K. Bachhuber, E. Buchner, and H. Hetzenauer, *Chem. Phys. Lett.* **165**, 369 (1990).
- <sup>66</sup>R. Brand, P. Lunkenheimer, U. Schneider, and A. Loidl, *Phys. Rev. B* **62**, 8878 (2000).
- <sup>67</sup>M. A. Miller, M. Jiménez-Ruiz, F. J. Bermejo, and N. O. Birge, *Phys. Rev. B* **57**, R13977 (1998).
- <sup>68</sup>M. Jiménez-Ruiz, M. A. Gonzáles, F. J. Bermejo, M. A. Miller, N. O. Birge, I. Cendoya, and A. Alegría, *Phys. Rev. B* **59**, 9155 (1999).
- <sup>69</sup>L. A. Leites, *Chem. Rev.* **92**, 279 (1992).
- <sup>70</sup>P. Lunkenheimer and A. Loidl, *J. Chem. Phys.* **104**, 4324 (1996).
- <sup>71</sup>R. H. Baughman, *J. Chem. Phys.* **53**, 3781 (1970).
- <sup>72</sup>E. C. Reynhardt and S. Froneman, *Mol. Phys.* **74**, 61 (1991).
- <sup>73</sup>Z. Gamba and B. M. Powell, *J. Chem. Phys.* **105**, 2436 (1996).
- <sup>74</sup>E. F. Westrum and S. Henriquez, *Mol. Cryst. Liq. Cryst.* **32**, 31 (1976).
- <sup>75</sup>P. Beckmann and A. Wendel, *J. Chem. Phys.* **73**, 3514 (1980).
- <sup>76</sup>O. Yamamuro (private communication).
- <sup>77</sup>The high-frequency deviations noted for ortho-carborane in Fig. 4 of Ref. 70 are of such kind.
- <sup>78</sup>P. Lunkenheimer, *Dielectric Spectroscopy of Glassy Dynamics* (Shaker Verlag, Aachen, 1999).
- <sup>79</sup>P. Lunkenheimer, A. Pimenov, M. Dressel, Yu. G. Goncharov, R. Böhmer, and A. Loidl, *Phys. Rev. Lett.* **77**, 318 (1996).
- <sup>80</sup>P. Lunkenheimer, A. Pimenov, M. Dressel, B. Gorshunov, U. Schneider, B. Schiener, R. Böhmer, and A. Loidl, *Mater. Res. Soc. Symp. Proc.* **455**, 47 (1997).
- <sup>81</sup>U. Schneider, P. Lunkenheimer, R. Brand, and A. Loidl, *J. Non-Cryst. Solids* **235–237**, 173 (1998).
- <sup>82</sup>For reviews on heterogeneity in glass-forming liquids, see: H. Sillescu, *J. Non-Cryst. Solids* **243**, 81 (1999); M. D. Ediger, *Annu. Rev. Phys. Chem.* **51**, 99 (2000).
- <sup>83</sup>L. Onsager, *J. Am. Chem. Soc.* **58**, 1486 (1936).
- <sup>84</sup>A. Schönhals, F. Kremer, A. Hofmann, E. W. Fischer, and E. Schlosser, *Phys. Rev. Lett.* **70**, 3459 (1993).
- <sup>85</sup>U. Schneider, P. Lunkenheimer, R. Brand, and A. Loidl, *Phys. Rev. E* **59**, 6924 (1999).
- <sup>86</sup>C. A. Angell, L. Boehm, M. Oguni, and D. L. Smith, *J. Mol. Liq.* **56**, 275 (1993).
- <sup>87</sup>C. A. Angell, *J. Phys. Chem. Solids* **49**, 863 (1988); R. Böhmer and C. A. Angell, in *Disorder Effects on Relaxational Processes*, edited by R. Richert and A. Blumen (Springer, Berlin, 1994), p. 11.
- <sup>88</sup>D. J. Plazek and K. L. Ngai, *Macromolecules* **24**, 1222 (1991).
- <sup>89</sup>R. Böhmer and C. A. Angell, *Phys. Rev. B* **45**, 10091 (1992).
- <sup>90</sup>W. T. Laughlin and D. R. Uhlmann, *J. Phys. Chem.* **76**, 2317 (1972).
- <sup>91</sup>C. A. Angell and W. Sichina, *Ann. N.Y. Acad. Sci.* **279**, 53 (1976).
- <sup>92</sup>R. Böhmer, K. L. Ngai, C. A. Angell, and D. J. Plazek, *J. Chem. Phys.* **99**, 4201 (1993).
- <sup>93</sup>Partly the results for  $m$  differ slightly from those reported earlier in literature (Ref. 92 and 98). However, our results can be assumed to be of higher precision as in general more data points were used for the determination of  $m$  from the Angell plot. The unusually small value of  $m$

- = 15 in phase I of adamantanone is based on a low-temperature extrapolation of  $\tau(T)$  and thus has a high uncertainty.
- <sup>94</sup>D. L. Leslie-Pelecky and N. O. Birge, *Phys. Rev. B* **50**, 13250 (1994).
- <sup>95</sup>J.-J. Pinvidic, S. Takahara, O. Yamamuro, and H. Suga, *Solid State Commun.* **72**, 501 (1989).
- <sup>96</sup>C. A. Angell, *J. Non-Cryst. Solids* **131–133**, 13 (1991).
- <sup>97</sup>P. Mondal, P. Lunkenheimer, R. Böhmer, A. Loidl, F. Gugenberger, P. Adelman, and C. Meingast, *J. Non-Cryst. Solids* **172–174**, 468 (1994); P. Mondal, P. Lunkenheimer, and A. Loidl, *Z. Phys. B: Condens. Matter* **99**, 527 (1996).
- <sup>98</sup>O. Yamamuro, M. Ishikawa, I. Kishimoto, J.-J. Pinvidic, and T. Matsuo, *J. Phys. Soc. Jpn.* **68**, 2969 (1999).
- <sup>99</sup>S. Benkhof, Ph.D. thesis, Universität Bayreuth, 1999.
- <sup>100</sup>G. Adam and J. H. Gibbs, *J. Chem. Phys.* **43**, 139 (1965).
- <sup>101</sup>G. P. Johari and M. Goldstein, *J. Chem. Phys.* **53**, 2372 (1970); G. P. Johari, *Ann. N.Y. Acad. Sci.* **279**, 117 (1976).
- <sup>102</sup>R. L. Leheny, N. Menon, and S. R. Nagel, *Europhys. Lett.* **36**, 473 (1996); A. Kudlik, T. Blochowicz, S. Benkhof, and E. Rössler, *ibid.* **36**, 475 (1996).
- <sup>103</sup>A. Schönhals, F. Kremer, and E. Schlosser, *Phys. Rev. Lett.* **67**, 999 (1991); N. Menon and S. R. Nagel, *ibid.* **71**, 4095 (1993); A. Schönhals, F. Kremer, and F. Stickel, *ibid.* **71**, 4096 (1993); A. Kudlik, S. Benkhof, R. Lenk, and E. Rössler, *ibid.* **32**, 511 (1995); Z. Dendzik, M. Paluch, Z. Gburski, and J. Ziolo, *J. Phys.: Condens. Matter* **9**, L339 (1997).
- <sup>104</sup>U. Schneider, R. Brand, P. Lunkenheimer, and A. Loidl, *Eur. Phys. J. E* **2**, 67 (2000).
- <sup>105</sup>N. B. Olsen, *J. Non-Cryst. Solids* **235–237**, 399 (1998); M. Jiménez-Ruiz, M. A. González, F. J. Bermejo, M. A. Miller, N. O. Birge, I. Cendoya, and A. Alegría, *Phys. Rev. B* **59**, 9155 (1999); C. León and K. L. Ngai, *J. Phys. Chem. B* **103**, 4045 (1999); H. Wagner and R. Richert, *J. Chem. Phys.* **110**, 11660 (1999).
- <sup>106</sup>P. Lunkenheimer, A. Pimenov, M. Dressel, Yu. G. Goncharov, R. Böhmer, and A. Loidl, *Phys. Rev. Lett.* **77**, 318 (1996); P. Lunkenheimer, A. Pimenov, and A. Loidl, *ibid.* **78**, 2995 (1997).
- <sup>107</sup>P. Lunkenheimer, R. Brand, U. Schneider, and A. Loidl, in *Slow Dynamics in Complex Systems: Eighth Tohwa University International Symposium*, edited by M. Tokuyama and I. Oppenheim, AIP Conf. Proc. No. 469 (AIP, New York, 1999), p. 671.
- <sup>108</sup>P. Lunkenheimer, R. Brand, U. Schneider, and A. Loidl, *Philos. Mag. B* **79**, 1945 (1999).
- <sup>109</sup>K. L. Ngai, *Phys. Rev. E* **57**, 7346 (1998); K. L. Ngai, *J. Chem. Phys.* **109**, 6982 (1998).
- <sup>110</sup>In Fig. 19, 1-cyanoadamantane is not included as no results on  $\beta_{\text{KWW}}(T_g)$  were available.
- <sup>111</sup>K. L. Ngai, *Comments Solid State Phys.* **9**, 127 (1979); K. L. Ngai, in *Disorder Effects on Relaxational Properties*, edited by R. Richert and A. Blumen (Springer, Berlin, 1994), p. 89.